Landmarks in Earth Reinforcement, - Ochiai et al (eds),
© 2003 Swets & Zeitlinger, Lisse, ISBN 90 265 1863 3

An outlook on recent research and development concerning long-term performance and extreme loading

Osamu Murata
Railway Technical Research Institute, Japan

ABSTRACT: This report describes about researches and developments of geosynthetic-reinforced soil retaining walls which use short planar geosynthetic reinforcement and a continuous rigid facing. Static loading tests with small models, long term observation of full scaled test embankments, static loading tests of full scaled test embankments, and shaking table tests were performed. The results of these tests showed that facing rigidity increases the stability of the wall remarkably. Considering these results, RRR method which is earth retaining wall with a relatively short geosynthetic and a rigid facing was proposed. RRR method has been used for important railway and road embankments and total length of the wall was about 50 km. During the 1995 Hyogoken-Nanbu Earthquake, RRR method with a total length 2km performed very well , though many conventional masonry, unreinforced gravity-type retaining walls and modern cantilever reinforced concrete retaining walls were seriously damaged.

1 INTRODUCTION

Railway Technical Research Institute in Japan has been studying geosynthetic-reinforced soil retaining walls since 1986.

In 1986 small models of reinforced earth retaining walls having different types of facing were failed by loading from the crest in laboratory. The results clearly showed that facing rigidity increases the stability of the wall remarkably.

From the end of 1987 through the beginning of 1988 two 5m-high full-scale test embankments were constructed. They had near-vertical slopes, reinforced with various types of short geosynthetics and facing. They had been observed their deformation under natural rainfall for one and a half year. And after observation of long term behavior, loading tests for two test embankments to failure were performed in 1989. The results also showed that walls with rigid facing were much more stable than walls with discrete panels.

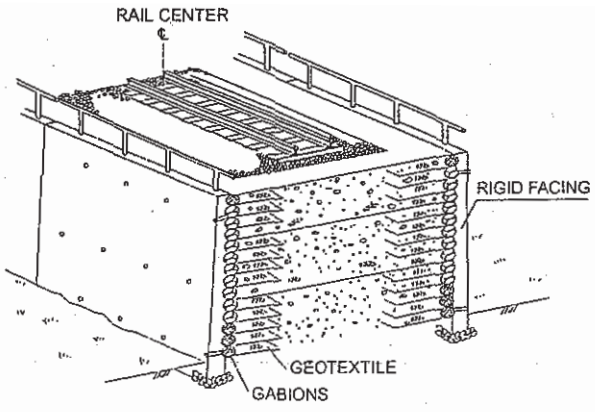

Fig.1 An artist view of the proposed method

In 1988 shaking table tests were performed. Compared to models having walls with discrete panels, models having walls with rigid facing were much more stable against seismic load.

Considering these results, RRR method (Fig.1) which is earth retaining wall with a relatively short geosynthetic and a rigid facing was proposed.

RRR method has already been used for almost 50km.

During the 1995 Hyogoken-Nanbu Earthquake, RRR method with a total length 2km performed very well, though many conventional masonry, unreinforced gravity-type retaining walls and modern cantilever reinforced concrete retaining walls were seriously damaged.

2 SMALL LABORATORY TESTS (Tatsuoka et al., 1989)

In order to define various different kinds of rigidities of the facing structures and their effects, a series of laboratory small model tests were performed using different facing structures(Fig.2, Table 1) .

Type D has a continuous rigid facing. Type C has a discrete panels facing with a rough back face. Type B has a discrete panels facing with a soft material in between vertical adjacent panels and a smooth back face so that the axial and shear forces and moment are not exerted in the facing. Type A has a rubber

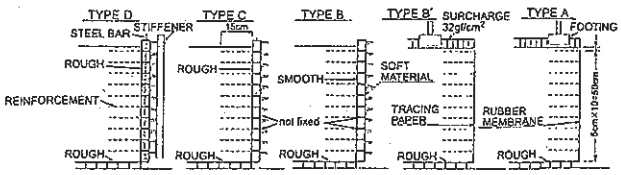

Fig.2 Small models of retaining walls having different types of facing used for laboratory tests

Table 1 Classification of facing types

FUNCTION OF FACING STRUCTURE	FACINGTYPE				
	A	B,B'	C	D	E
LOCAL RIGIDITY	NO	YES	YES	YES	YES
OVERALL VERTICAL RIGIDITY	NO	NO	YES	YES	YES
OVERALL BENDING STIFFNESS	NO	NO	NO	YES	YES
RESISTANCE BY VALL VEIGHT	NO	NO	NO	NO	YES

membrane facing. For each facing type, the wall was loaded with a 10cm-wide footing having a smooth base.

The model grid reinforcement was designed not to rupture in tension. The length was 15cm (only 30% of the wall height).

Fig.3 is a summary showing the results for the above four types of facing.

In Fig.3, q_u is the ultimate average footing pressure when the footing was placed on the crest of reinforced zone. Type D had much larger qu (67.8kN/m2) than Type C (qu:28.0kN/m2), Type B(qu:12.3kN/m2), Type A(qu:3.50kN/m2).

The local footing pressure q for the two halves of

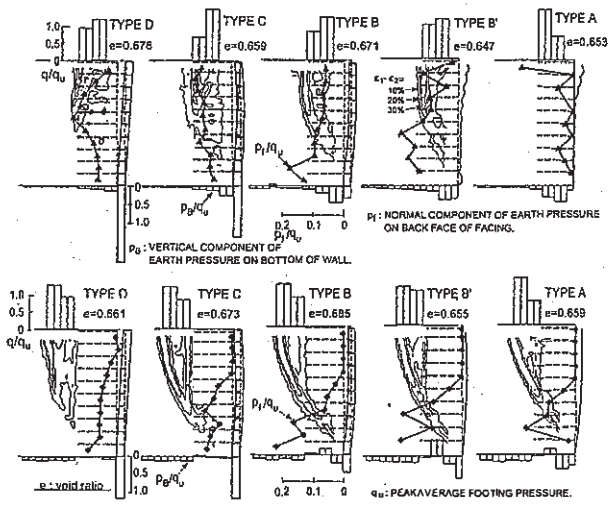

Fig.3 Pressure distributions on bottom face of footing(P_B/q_u) and the back surface of facing(P_f/q_u) (normalized by being devided by the maximum average footing pressure q_u), the deformation pattern of facing and the strain field in the backfill, at the moment of the peak footing pressure; (a) Front loading, (b)back loading. The pressure values are increments due to loading with footing.

footing and the earth pressure on the back face of the facing, the bottom of the wall(pF and pB) are divided by qu. The values of P_f and P_b are due to the footing pressure.

The contour lines show local shear strain ε1-ε3 (%) observed at the failure.

It may be seen that the wall became more stable as the facing rigidity increased and pressure working at the back face and the bottom of the facing increased as the facing rigidity increased. This means that larger part of the weight of the back fill and footing load can be supported by the facing with adequate rigidity and thereby the resistance of wall against overturning and sliding out increases.

3 CONSTRUCTION AND LOADING TESTS OF JR NOS.1 AND 2 TEST EMBANKMENT

3.1 Construction of JR test embankments (Tatsuoka et al.,1992)

Two full-scale test embankments were constructed from the end of 1988 through the beginning of 1989.

For the backfill material, a sand having a mean diameter of 0.2mm and a fines contents of 16% was used for the first test embankment (JR No.1 embankment) and Kanto loam having an initial water content of 120-130% and an initial degree of saturation of about 90% and a dry density of 0.55-0.60 g/cm^3 was used for the second embankment (JR No.2 embankment).

Figs.4(a) and 5(a) show their plans and Figs.4(b) and 5(b) show three cross-sections of each embankment, in which the solid lines show the dimensions at the end of construction and the broken lines show those after about two years had elapsed(in February 1989). Note that the scales for the embankments and the deformation differ 60 times. Each cross-section had two test wall segments.

The sand embankment(JR No.1 embankment) was reinforced with a grid which consisted of members made of polyester with a rectangular cross-section of 0.9 mm × 3mm and an aperture of 20 mm, covered with PVC to increase its durability. It had a tensile rupture strength of 28 kN/m and an initial tensile modulus of 10 kN/m at an elongation of 5%, which were measured by tensile loading tests at a strain rate of 5%/min. The vertical spacing between reinforcement layers was 30 cm and the length was 2.0 m, except 1.5 m for segment f.

JR No.1 test embankment had six test walls. Among them, five walls had a continuous rigid facing of delayed cast-in-place unreinforced concrete and one had a facing of discrete panels covering the wrapped-around wall face which were constructed with the aid of gabions. Each discrete panel had an area of 0.6 m × 0.6 m and a mass of 40kg.

JR No.2 clay test embankment also had six test walls, all of which had a continuous rigid facing. In all the cross-sections, the vertical spacing between

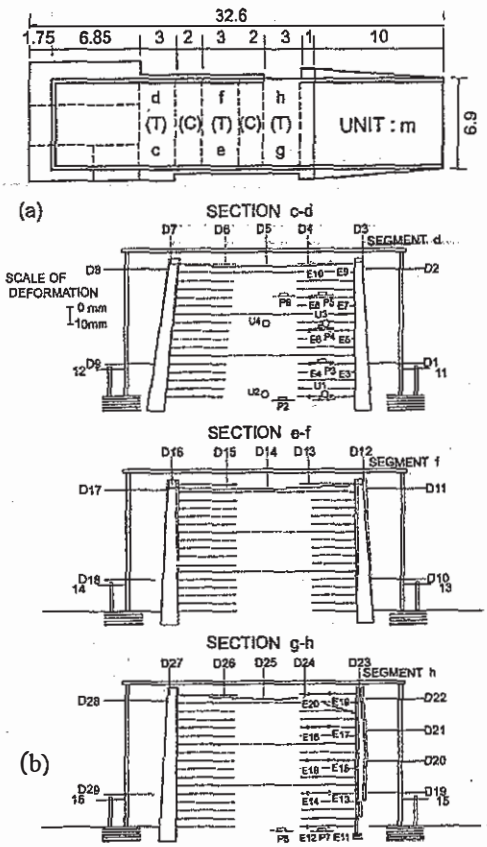

Fig.4 (a) Plan and (b) three sections of JR No.1 embankment (sand) (T; test section, and C; control section)

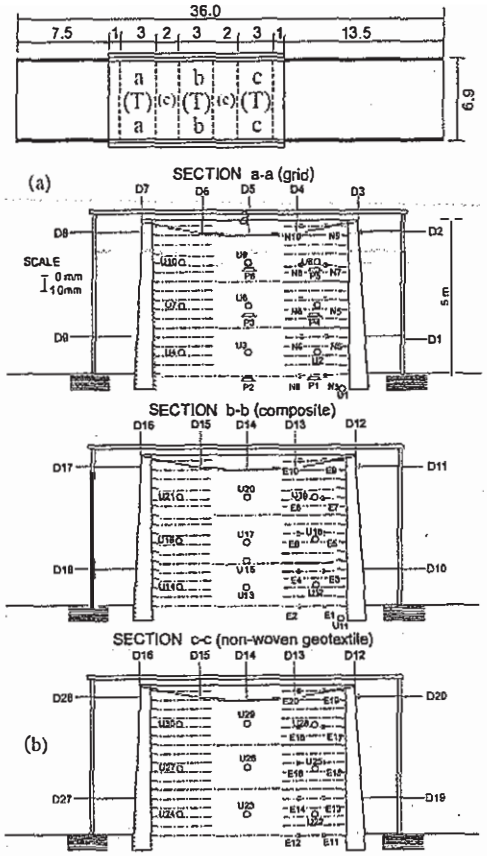

Fig.5 (a) Plan and (b) three sections of JR No.2 embankment (clay) (T; test section, and C; control section)

reinforcement layers was 30 cm and the length of reinforcement was 2.0 m. The two test wall segments in section a-a were reinforced with a grid as in JR No.1 embankment. Each grid sheet was sandwiched between gravel drainage layers. Section b-b used a non-woven geotextile with a rupture strength of 7 kN/m. Section c-c used a composite of high tensile-rigidity woven geotextile sandwiched in between two non-woven geotextile sheets. The composite had a rupture strength of 18 kN/m and an initial tensile modulus of 14 kN/m at 5% strain.

The long-term behavior of the two embankments are shown in Fig.6. It may be seen that all the test wall segments having a continuous rigid facing exhibited a very small settlement of 1 cm or less even at the center of crest over one and a half years after the construction (see also Figs. 4(b) and 5(b)). Compared to that, only segment h having a discrete-panel facing of JR No.1 deformed much larger, associating with relatively large tensile strain in the reinforcements(see Fig.6(a)).

The effect of facing type shown above was well in agreement the laboratory model test results shown in Fig.3.

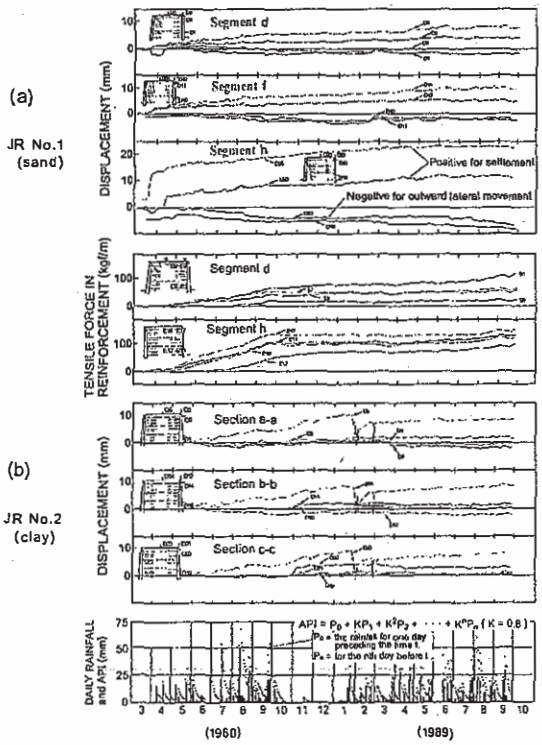

Fig.6 Long-term behavior of (a) JR No.1 embankment (sand), and (b) JR No.2 embankment (clay)

3.2 Loading tests to failure(Tatsuoka et al., 1992)

Three sections of JR No.1 test embankment were loaded at their crests using a 2 m×3 m footing by the method shown in Fig.7. The 3 m-wide test sections were separated from each other by a 2 m-wide control section in between (see Fig.4(a)). A layer of two plywood sheets sandwiching a layer of grease had been placed to lubricate the planes between each test section (denoted as 'T' in Figs.4(a) and 5(a)) and the control sections (denoted as 'C' in Figs.4(a) and 5(a)) in order to achieve plane strain conditions. The footing was located at a setback of 2 m from the edge of the crest of segments d, f and h.

The results are presented in Fig.8, 9 and 10.The effect of the different length of geotextile between Segments d and f (2.0 m and 1.5 m) and the effect of the different facing types between Segments d and h may be seen clearly in Figs. 8 and 9. The lower part of the discrete-panel buckled during the loading test, due to the fact that the facing could not resist the axial force caused by the footing load.

From the observation during the loading tests, it was found the Segments d and f yielded when a crack appeared in the upper construction joint (see Figs 8 and 9). It seems, therefore, that if the construction joints had been stronger, the strength of the walls would have been larger. Indeed, the behavior shows the important role of the overall rigidity of facing for the stability.

Following the loading tests for JR No.1 embankment, one section of JR No.2 embankment(Section c-c) reinforced with the composite geotextile was loaded from its crest. In this case, the loading tests were performed in the following two phases. The first phase loading was applied near the center of crest, slightly closer to the left-hand side wall using a footing with a 2 m × 3 m base by the method of back loading as used for JR No.1 embankment shown in Fig.7. The first phase loading was ceased before the

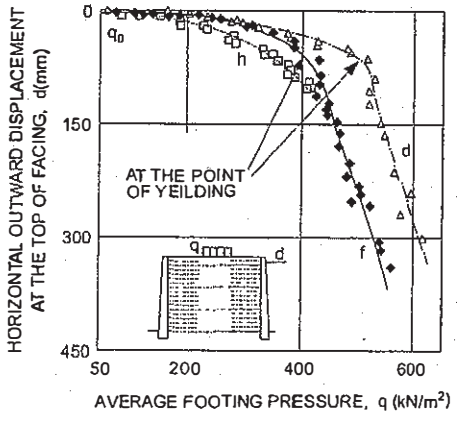

Fig.9 Load-displacement relations for Segment d, f and h of JR No.1 embankment by loading test; q_0: the average pressure due to the weight of the loading apparatus(=50kN/mm^2)

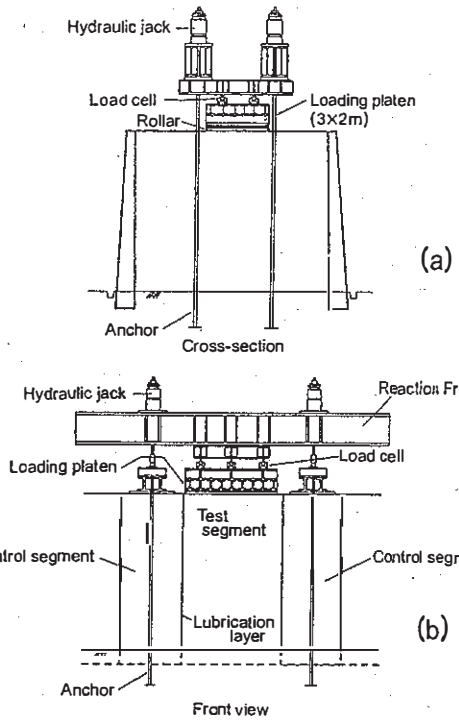

Fig.7 Loading method used for JR No.1 test embankment

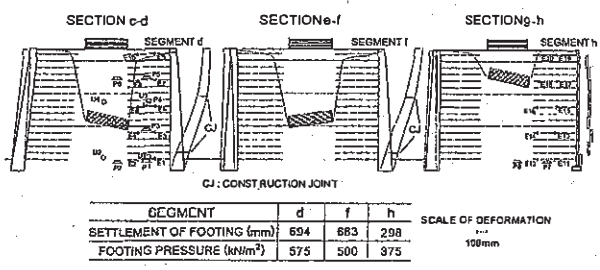

Fig.8 Deformation of three sections of JR No.1 test embankment by loading test

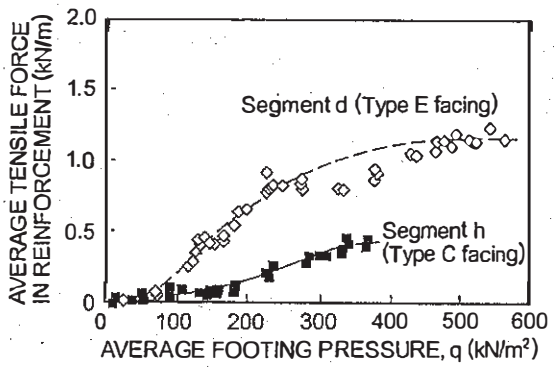

Fig.10 Average tensile strain developed due to loading, JR No.1 embankment

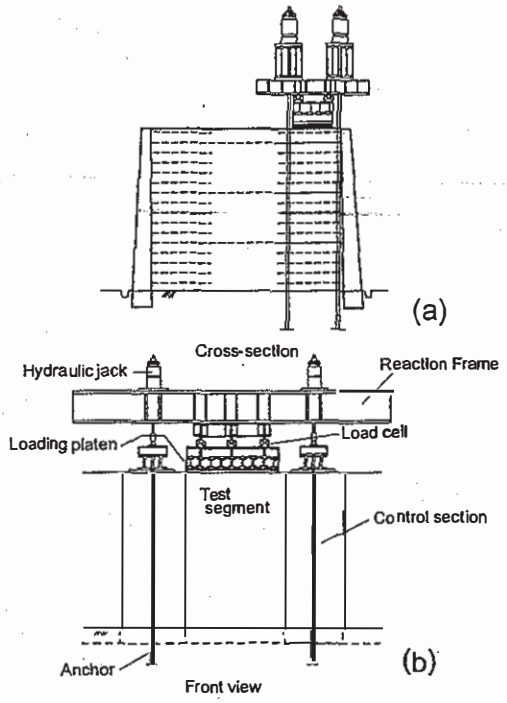

Fig.11 Front loading method for JR No.2 embankment

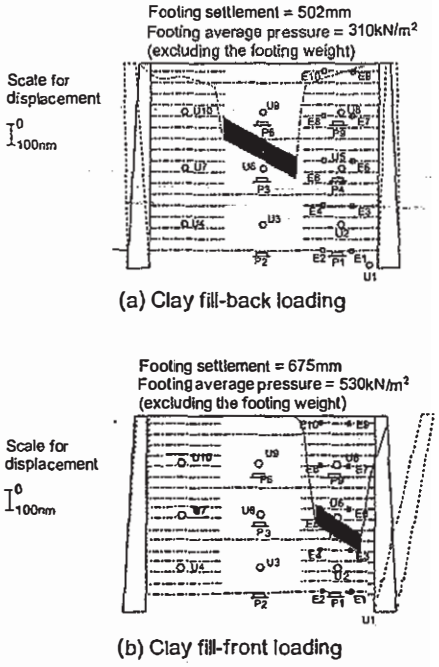

Fig.12 Deformation of JR No.2 embankment by loading test: (a) back loading, and (b) front loading

wall was damaged too much in order not to influence the second phase loading test. Subsequently, as shown in Fig.11, from the top of the right-hand side reinforced zone, the second phase loading was applied using a footing with a 1 m × 3 m base (front loading). Before these tests, the delayed cast-in-place concrete facing of the right-hand side wall was supported on the outer face by using a stiffener (I-shaped steel beams) so that the construction joint will not yield during the loading test.

The test results are shown in Fig.12 through 15. It may be seen from Fig.13 that for the back loading, the clay fill was not as strong as Test wall segment d of the JR No.1 sand embankment. It is to be noted that this clay wall is yet strong enough, considering that the design pressure by train weight is only about 30 kN/m^2. It may also be seen from Fig.13 that the clay wall is stronger against loading from the crest (front loading) than against the back loading. This tendency is the same as the observed in the laboratory tests.

Fig.14 shows a very interesting record of pore pressure in JR No.2 clay embankment. It may be seen that the pore pressure increased due to loading in both cases. However, the dissipation of the excess pore water pressure was much faster in the case of front loading than in the case of back loading. It was because in the case of front loading, the composite geotextile drained the excess pore pressure built-up near the point of recording very effectively, although it was not the case in the case for the back loading, in which the loaded zone was not reinforced with the composite geotextile. This result indicates that the

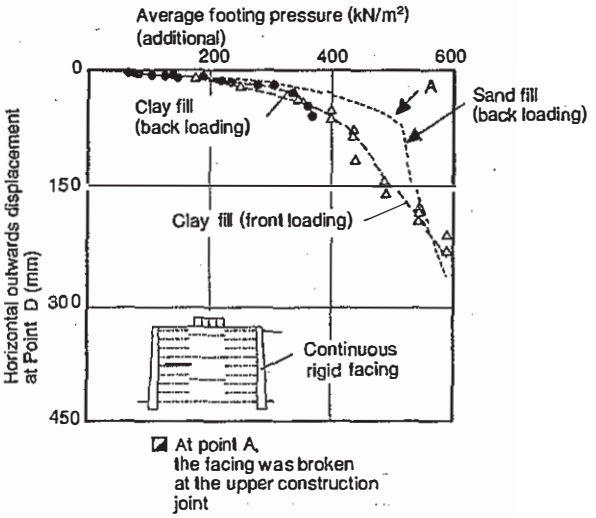

Fig.13 Load-displacement relations for clay fill JR No.2 embankment by back loading and front loading, in comparison of those for sand fill JR No.1 embankment, Segment d.

use of geotextile having a function of drainage can increase the shear strength of saturated or near-saturated clay upon loading.

Fig.15 shows the creep settlement of footing on the clay wall during sustained loading for about 22 hours for both cases of the back and front loading as shown in Fig.14. It may be seen that the rate of creep deformation decreased rapidly in spite of the relatively large footing pressure of about 200 kN/m^2.

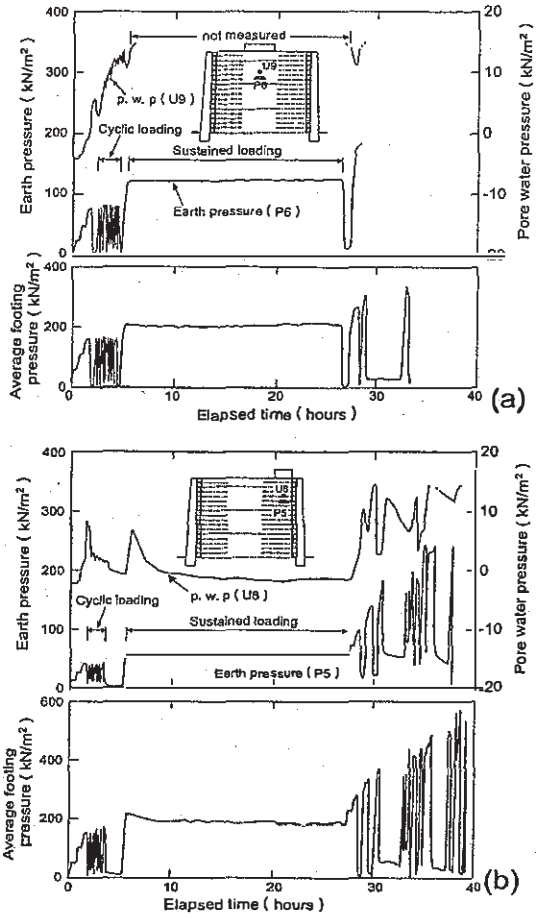

Fig.14 Time histories of earth pressure, pore pressure and footing average pressure in JR No.2 embankment; (a) back loading, and (b) front loading

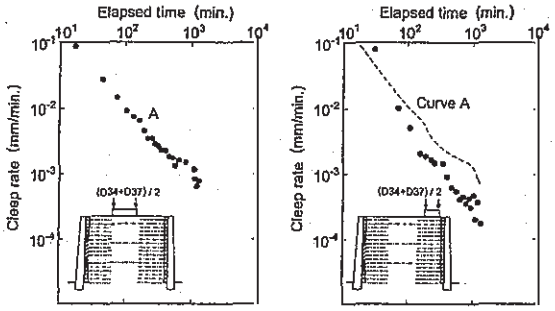

Loading phase	Loading period (hrs)	Settlement of footing (mm)	Outwards displacement at the top of facing (mm)	Tensile strain in reinforcement (%)
Back	2.2	7.09	0.47	0.56
Front	22.5	3.33	0.87	0.53

Fig.15 Creep behavior of JR No.2 embankment during sustained loading: (a) back loading, (b) front loading

4 SHAKING TABLE TESTS BEFORE THE 1995 HYOGOKEN-NANNBU EARTHQUAKE

4.1 Small model tests (Murata et al.,1992)

A series of shaking table tests of 100 cm-high scaled models were performed to ascertain a seismic design (Fig.16). The sand backfill was reinforced with a grid having a high rupture strength of 10 kN/m, which leaded to no chance of rupture during the model tests.

Case 1 was the standard one having a vertical continuous rigid facing (Type D :Fig2).

Compared to Case 1, Case 5 had a discrete panel facing (Type B: Fig2), Case 2 had longer reinforcement, Case 3 had an inclined facing and Case 4 had a smaller number of reinforcement layers. A series of horizontal shaking at a constant amplitude of acceleration was applied with increasing the acceleration level step by step.

The accumulated horizontal outward displacement of facing at the end of each step of shaking was much larger for Case 5 than for Case 1 (Fig.17), apparently due to its low facing rigidity. The wall also became more stable by using longer reinforcement (Case 2) and by using an inclined facing (Case 3), but became less stable by using a smaller number of reinforcement layers (Case 4).

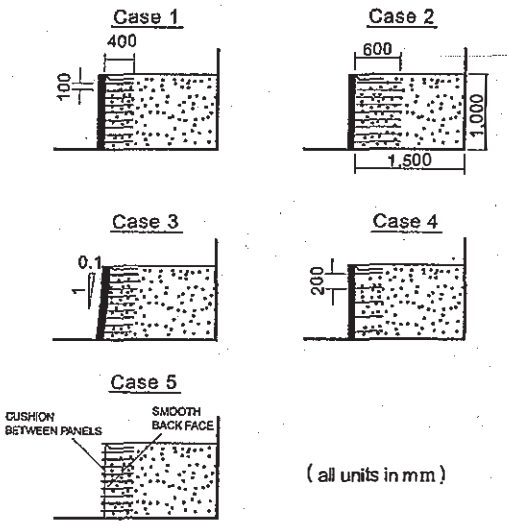

Case	facing	NRL*	LR*	Slope of wall face	Note
1	one unit	10	400mm	Vertical	Standard
2	one unit	10	600mm	Vertical	Longer reinforcement
3	one unit	10	400mm	1 : 0.1 (V:I)	Inclined facing
4	one unit	5	400mm	Vertical	Smaller NRL
5	discrete	10	400mm	Vertical	Less rigid facing

NRL : Number of reinforcement layers
L R : Length of reinforcement

Fig.16 Models for dynamic loading tests

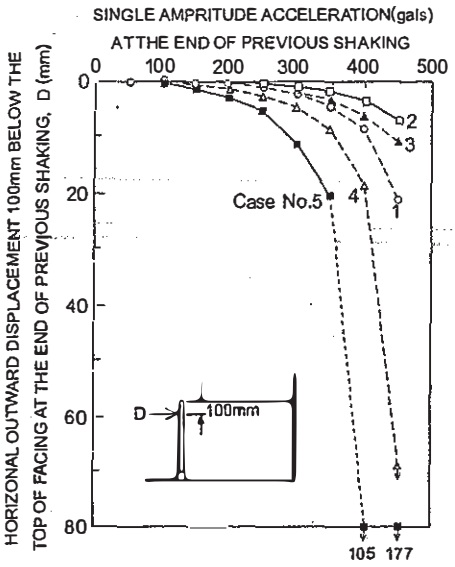

Fig.17 Results of dynamic tests (Fig.16)

4.2 Large Model Tests (Murata et al.,1992)

After small scale shaking table tests, a 248 cm-high model, of which the scale is a half of the field prototype, was constructed on a large shaking table. Then, a series of shaking tests were performed in order to confirm the resistance capacity against earthquake load.

The wall height in the model was 248 cm and its width was 345 cm (Fig.18). The backfill and reinforcement material were essentially the same as those used for JR No.1 test embankment with sand backfill. However, the scale was reduced to a half of the field prototype.

The model wall was constructed in a large steel sand box with a width of 3.0 m, as follows:

1) The base ground was placed using appropriate compaction (Table 2). The relative density was 58.4% (relatively loose state).
2) The wall was constructed in the same way as the prototype (also as the actual walls: Fig.22). The sand was compacted by using a small compactor at lifts of 15cm utilizing gabions at the edge of each soil layer (Table 2). The grid reinforcement used had a tensile rupture strength of 10 kN/m, one third of that of the grid used for JR No.1 test embankment. When the similitude rule is applied, the strength of the grid should be about one fourth of the strength of the prototype grid. However, such a grid was not available. The aperture of the grid was 20mm by 20 mm, and the length was 1.0 m, about 40% of the wall height, except for three full-width layers (see Fig.18).
3) The slope of the completed wall face was 1.0:0.05 (V:H). The sides of the facing were about 1 cm from the steel sand box.

The shaking table tests had the following three phases.

(1)Vibration test A:

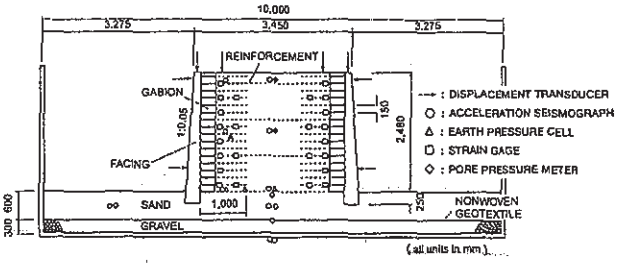

Fig.18 Configuration of large scale model and instrumentation

Table 2 Index propeties of soils

	Wet density ρ_t (g/cm³)	Dry density ρ_d (g/cm³)	Water content w (%)	Degree of compaction (%)
Backfill	1.82	1.60	13.7	90.4 *
Ground	1.57	1.54	2.1	58.4‡

* : Relative density:

Nine stages of horizontal sinusoidal motion, at a frequency of 3.4 Hz, were applied to the shaking table for a duration of 20 seconds. At each step, the acceleration was increased by 50 gals (= cm/sec^2), from 100 gals to 500 gals.

(2)Vibration test B:

A time history of earthquake motion (horizontal component), recorded at the ground surface during a major earthquake in the past, was applied after having being adjusted to a predominant frequency of 2.45 Hz (considering the similitude rule) and a maximum acceleration of 500 gals. The application period was 2 minutes.

(3)Vibration test C (Liquefaction test) :

After saturating the supporting sand layer, two steps of sinusoidal motion, at a frequency of 2.0 Hz and with a maximum acceleration of 200 and 400 gals, were applied to the shaking table for a duration of three minutes. In this test, the supporting sand layer liquefied.

Many measuring instruments located in the backfill and the supporting ground, were set to observe the behavior of the model during the vibration tests (see Fig.18).

Fig.19 shows the amplification ratio of the maximum acceleration along the vertical direction in the reinforced zone and at the center of the wall during Vibration tests A and C. In vibration test A, almost no amplification was observed up to the mid-height of the wall, while it was still less than 1.5 times at the crest. Further, the behavior was very similar for the reinforced zone and the central unreinforced zone. These results suggest that the wall exhibited an approximately monolith behavior. The behavior during Vibration test C (liquefaction test) was similar, but the amplification was slightly larger. All these results indicate positive effects of reinforcement combined

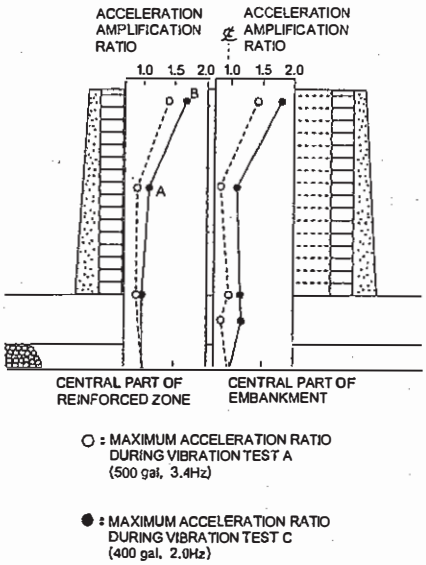

Fig.19 Acceleration amplification ratio in the embankment

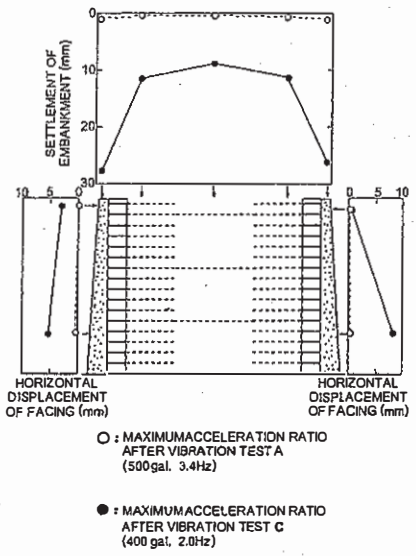

Fig.20 Maximum deformation of the embankment after vibration

with rigid facing.

Fig.20 shows the outward lateral displacement at the wall face and the settlement at the wall crest observed after the loading at 500 gals in Vibration test A and the loading at 400 gals in Vibration test C. It may be seen that even very large dynamic load was applied, while failure did not occur in the supporting ground (Vibration test A), the deformation of the wall was very small (the outward deformation displacement at the top of facing was only 1.0 mm). Fig.21 shows the maximum reinforcement tensile forces during vibration compared with those before vibration. It may be seen that the increase during vibration was very small compared to the tensile force under the static condition. The maximum value during vibration was much smaller than the rupture strength of the reinforcement.

The increase in the deformation of the wall by Vibration test B using an amplified earthquake motion was smaller than that occurring by Vibration test A. The behavior of the model wall during Vibration tests A and B indicates that this RRR method could be very stable even during strong earthquake.

Vibration test C was very special test, since prototype walls should never be constructed on a liquefiable soil deposit. That is, such a soil deposit will first be improved by some means before constructing. This test was performed to verify if the wall bearing capacity of the facing is lost. It may be seen from Fig.20 that the maximum settlement observed at the crest after the test was about 11 mm and 28 mm at the center of the crest and the facing, respectively. The maximum outward lateral displacement of the facing was about 8 mm near the wall bottom. This rather large deformation occurred due to the lost of the bearing capacity of the supporting ground during liquefaction. It is to be noted that in spite of this relatively large deformation, the entire wall moved just as a monolith and was very stable. It was confirmed after taking the wall apart that the connection between the facing and the reinforcement was not damaged at all. This is despite a rather large relative movement between the facing and the backfill (about 20 mm). It is likely that the stack of gabions acted as a buffer zone. It may be seen from Fig.21 that the increase in the tensile force in the reinforcement layers during dynamic loading was slightly larger than that during Vibration test A. It seems that this relatively large increase was mainly due to the relative settlement of the facing (see Fig.20).

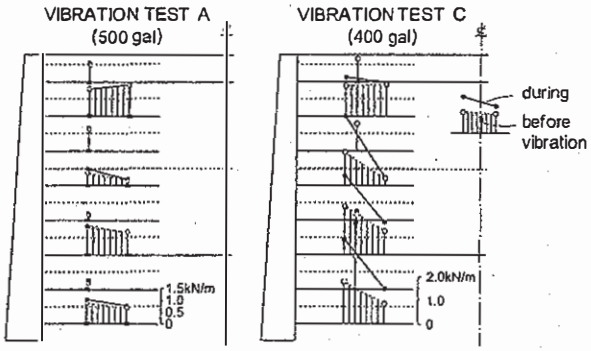

Fig.21 Maximum reinforcement tensile force during vibration

It should be noted that the tensile force in the three full-width reinforcement layers during Vibration tests A and C (also test B) was not particularly large when compared with those in the other layers (see Fig.20). These results show that connecting both faces with these three layers did not contribute much to increase the stability of the wall during the dynamic loading tests.

5 THE PROPOSED SOIL-REINFORCING METHOD (Tatsuoka et al.,1992)

Based on the results of the laboratory model tests, their long-term behavior and the results of the loading test, and the results of the shaking table tests, together with the results of stability analysis by the limit equilibrium method, the following method of the soil-reinforcing method (RRR method) was proposed. Fig.22 shows the standard construction method of RRR method. Namely, first a base RC leveling pad is constructed. Then, the first geosynthetic layer is placed followed by setting gravel bags (gabions) at the shoulder, over which the geosynthetic sheet is rolled over. The first soil layer is placed on the geosynthetic sheet and compacted very densely. The second layer (geosynthetic plus soil) is similar to the first layer, and this procedure is repeated until the full wall height is completed. After the deformation and settlement of the wall and the supporting ground is ceased, a lightly steel-reinforced concrete layer is cast-in-place directly on the geosynthetic without using a framework for casting concrete on the wall face.

The characteristic features of this method may be summarized as follows:

(1) the use of planar geosynthetic sheets,
(2) the use of relatively short reinforcement sheets,
(3) the use of a continuous rigid facing, and
(4) the stage-construction method

Planar geosynthetic sheets are used to reduce the required anchorage length by increasing the contact area with the backfill, as compared to the use of metal strips.

Relatively short reinforcement sheets with a length of, say, 30% -40% of the wall height are used so that it can be used for the reconstruction of embankment as shown in Fig.23. It has been confirmed experimentally that the reduction in the stability of wall by using a planar geosynthetics and using a continuous rigid facing.

A continuous rigid facing is placed directly over the wrapped-around wall face for the purpose of increasing the stability of wall and for reducing the lateral and vertical deformation at the wall face and the settlement of the backfill, by enhancing the reinforced zone and the facing together to behave like a monolith. Its use also increases the resistance against mechanical and fire damage of the reinforcement, and avoids the deterioration of geosynthetics when exposed to ultraviolet light. It becomes also possible by using a rigid facing to produce a good appearance of wall face by, for example, creating a decorated pattern on the wall face.

The stage construction method is employed to alleviate the following potential problems associated with the use of a continuous rigid facing:

(1) The connection between reinforcing members and facing may be damaged due to the relative settlement between them.
(2) Only small tensile strains may be mobilized in reinforcing members when soil layers are compacted as a continuous rigid facing is firmly propped.

Large earth pressure may be activated on the back face of facing due to the compaction of backfill as a continuous rigid facing is firmly propped.

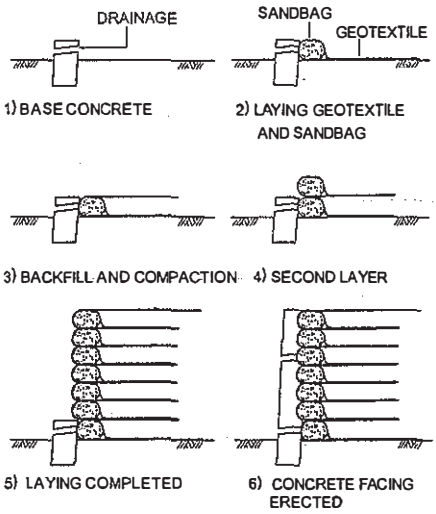

Fig.22 Standard construction procedure of RRR method

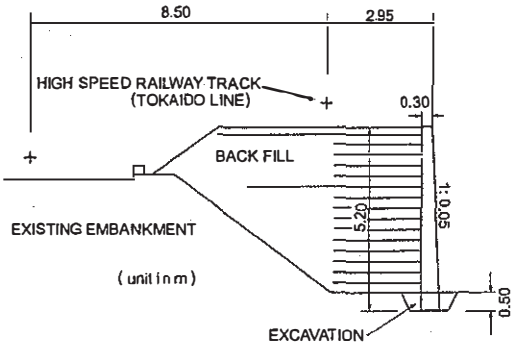

Fig.23 Typical cross-section of the slope of railway embankment for Tokaido Line reconstructed by the proposed geosynthetic-reinforced soil retaining wall method (RRR method), Amagasaki

6 ACTUAL APPLICATION OF THE PROPOSED SOIL-REINFORCING METHOD

The first actual application of the proposed soil-reinforcing method (RRR method) in the preceding sections was the reconstruction of existing railway embankments of Japan Railway companies in 1988 in Shikoku Island (wall height: 0.9-3.0m and wall length: 70m) and in 1989 in Ten-noji, Osaka (wall height: 1.8m and total wall length: 20m). These two cases were relatively small-scale.

The application in a large scale construction was at three sites described bellow, starting in 1989 and 1990. To the best knowledge of the author, these applications of soil-reinforcing method for permanent important railway was the first in the world. And in 1996, RRR method was applied to train yard site which was constructed on the very weak ground in Nagano. Now the total length of RRR method is more than 50 km.

6.1 Nagoya Bullet Train Yard Sites (Tateyama et al., 1994)

RRR method was constructed for expanding the area of the yard for the bullet train (Shinkansen) at Hibitsu in Nagoya City. The existing of embankment for a total length of 930 m, with an average height of 5 m, was reconstructed to near vertical retaining walls. The construction was started in 1990 and completed in 1991.

Fig.24 shows a typical cross-section of RRR method of this project. Since most part of the wall face was next to public roads and close to nearby residential areas, it was made aesthetically pleasing by forming the appearance of natural stone using cast-in-place concrete together with special concrete framework. Fig.25 shows two bridge abutments by RRR method supporting a railway bridge girder. Considering its critical use, a relatively strong grid with a tensile rupture strength of 60 KN/m was used. As backfill soil, a well grained sandstone gravel used and compacted very well to a dry density of as high as about 2.2 g/cm^3.

The stability analysis of the bridge abutments for lateral sliding and overturning was performed by limit-equilibrium methods (Horii et al.,1994). In the static loading test performed immediately after the completion of the wall construction, a total pressure of 400 kN and an average pressure of 20 kN/m^2, which was similar to the design train load, was applied to the concrete block on one of the bridge abutments (the left-side in Fig.25). The settlement was only 0.1 mm.

Trains started passing on the bridge on 29th October 1992. The long-term behavior of the abutment on which the above-mentioned static loading tests were performed has been monitored continuously since the completion of the wall construction.

As shown in Fig.26, precipitation, strains in the reinforcement, vertical earth pressure, pore water pressure and settlement in the backfill, strains in the steel reinforcement in the rigid facing and its tilting at the wall face were measured. The locations of the settlement gauges, the reinforcement strain gauges are also indicated in Fig.25(d).

The dynamic behavior of the abutment during train passing was also recorded. In addition to those shown in Fig.26, the rail strain and acceleration at the crest of the abutment were recorded by means of a data recorder.

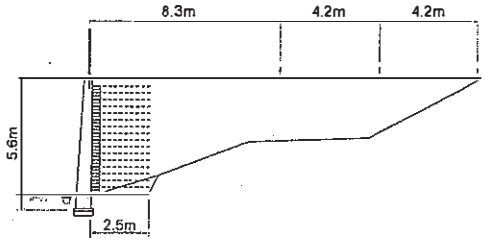

Fig.24 Typical cross-section of RRR method at Hibitsu, Nagoya

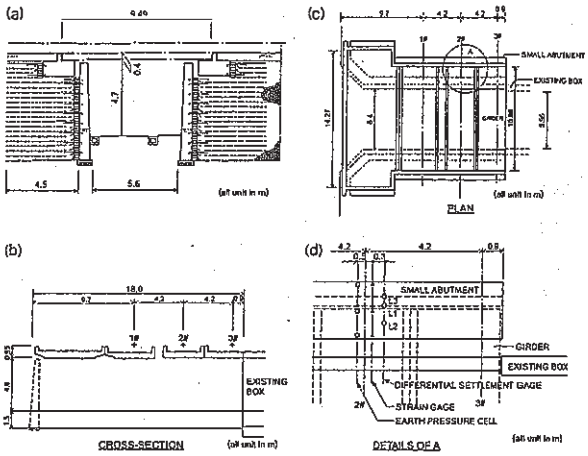

Fig.25 Bridge abutments at Hibitsu, Nagoya; (a) front view, (b) cross-section, (c) plan and (d) close view of zone A in (c)

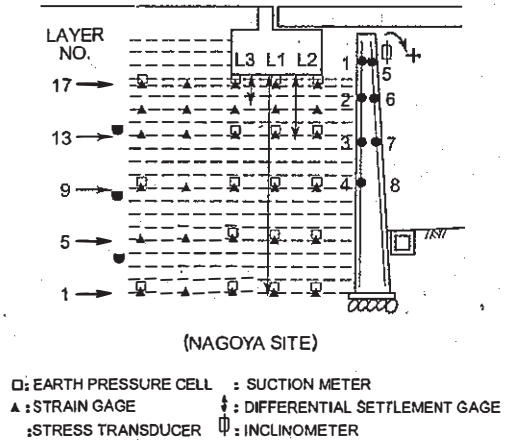

Fig.26 Arrangement of measuring instrumentation in the bridge abutment at Hibitsu, Nagoya

The behavior of the bridge abutments was observed for 1.5 years from September 1991 until February 1993. The general trend is that the compression of the backfill increased correspondingly to the precipitation, probably due to the reduction in suction by rainfall. But the total settlement was very small (about 2.0 mm). The settlement due to dynamic train loads can also be noticed. However, the rate of the

vertical compression decreased with time and about two months after opening to train passing, the increase in the settlement virtually ceased. The total settlement at the concrete block on the crest of the abutment since traffic started was 2.0 mm.

On October 29th 1992, the first train of Shinkansen passed above the abutment at a velocity of about 9 km/h. The wheel load was 160 kN. Fig.27 shows the time histories of several typical measurements during train passage. These values are in increments caused by the train load. It may be seen from Fig.27(b),(c) that due to the relatively low velocity, the horizontal and vertical acceleration on the crest of the abutment were very low.

The correspondence between the vertical earth pressure and the reinforcement tensile strain shown in Figs.27(d-1) and (d-2) is very obvious, but it does not apply to other cases in Fig.27. The same tendency was observed among the corresponding cases during the static loading test. In any case, the change in the reinforcement force is very small with maximum tensile force of only 50 N/m.

It may be seen from Fig.27(d-1),(e-1) and (f-1) that the maximum earth pressure at the measuring point closest to the facing in the soil layer No.17 was smaller than those measured at more remote points. This behavior was also observed when a train supported on the abutment as shown in Fig.28. This result may suggest that it was sufficiently large, the degree of restraint against outward lateral spreading of soil by tensile reinforcement with the help of a rigid facing was not as large as it is at level ground of reinforced dense gravel. Yet, the degree of this non-uniform earth pressure was very small and did not lead to any problem.

It may also be seen in Fig.28 that the increase in the vertical earth pressure at the wall base due to train load decreased to about half of that measured immediately below the concrete block. When this earth pressure is modeled by a uniform increase in the zone between the back face of the facing and a plane radiating from the heel of the concrete block, the distribution angle becomes 27^0 relative to the vertical.

It may be seen from Fig.27(h) that the vertical compressional strains in the backfill soil below the concrete block was very small. The settlement of the concrete block as measured at L2 was about 0.05 mm, which was extremely small; this value was much smaller than the 5 mm allowable maximum settlement of the track during train passing. This value was

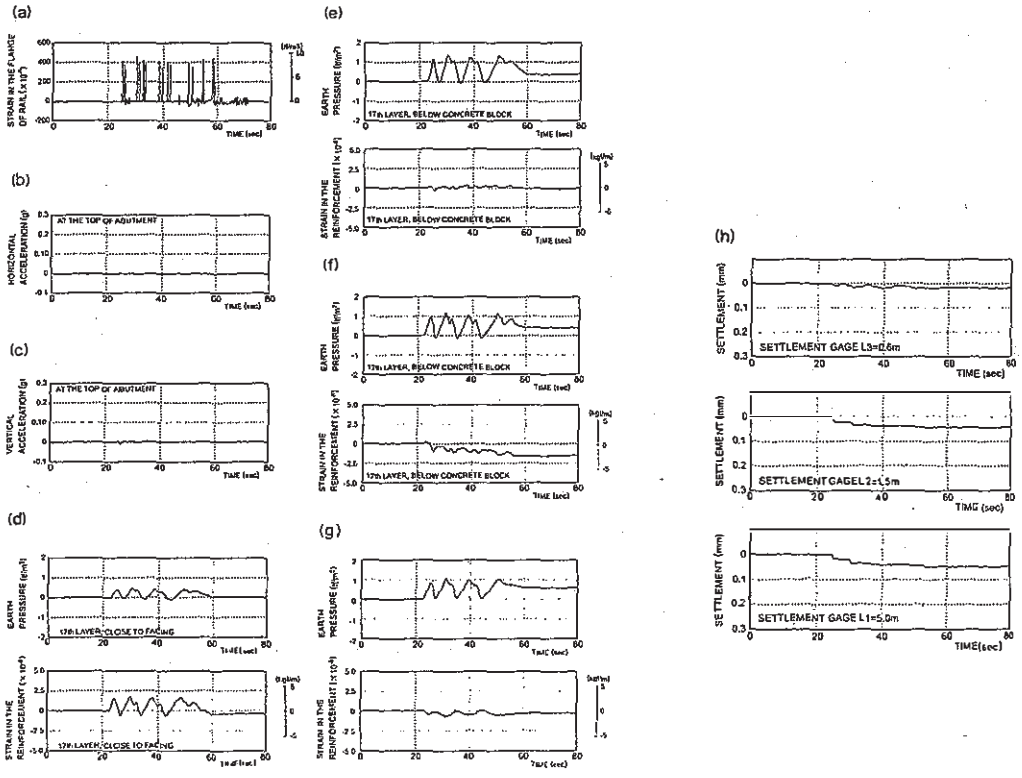

Fig.27 Time histories during the first passing of train on October 29 1992 of the changes in: (a) strain in the flange of rail, (b) and (c) horizontal and vertical acceleration on the crest of the GRS-RW abutment, (d-1) and (d-2)~(f-1) and (f-2) pairs of vertical earth pressure and reinforcement tensile force in the soil layer No.17, (g-1) and (g-2) a pair of vertical earth pressure and reinforcement tensile force in the soil layer No.17 , (h-1)~(h-3) vertical compression in the backfill below the concrete block at L1, L2 and L3 (gauge lengths=5m, 1.5m and 0.6m) (see Figs, 4 and 6 for the locations of measuring instrumentation)

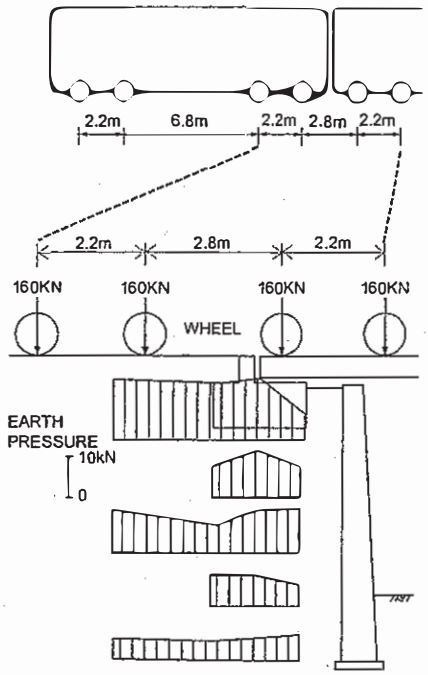

Fig.28 Typical record of earth pressure when a train stopped on the GRS-RW abutment

slightly smaller than that observed during the static loading test (=0.1 mm).

Observations and measurements showed that the bridge abutments (and ordinary part of RRR method walls) have been very stable without showing noticeable deformation.

6.2 Amagasaki Tohkaido-Line Site (Kanazawa et al.,1994)

Fig.29 shows the typical cross-section of the RRR method. The average wall height was 5 m and the total wall length was 1,300 m. The construction of the RRR method was started in October 1990, and ended in August 1991. The tracks were open for traffic in December 1991.

Soil used for the backfill is mostly borrowed sand for the ordinary retaining wall sections, while a well-graded gravel of crushed sandstone having D_{50}=10.8 mm and a uniformity coefficient U_c=12.5 was used for the bridge abutments. The backfill soil was mechanically compacted to a dry density of around 20 ~21 kN/m^3.

In place of the ordinary type of sand bags made of steel grid, metal-wire mesh gabion (bag) as shown in Fig.30 was used to minimize labor. The length of one unit bag is 1.8 m. A metal-wire mesh bag was first placed on the shoulder of each soil layer, in which subsequently gravel was placed. Then, a non-woven geotextile sheet was wrapped around each bag to protect the geosynthetic reinforcement, which was then wrapped around the bag.

At three locations, the railway has an over-bridge over a road. Table 3 was prepared for selecting the

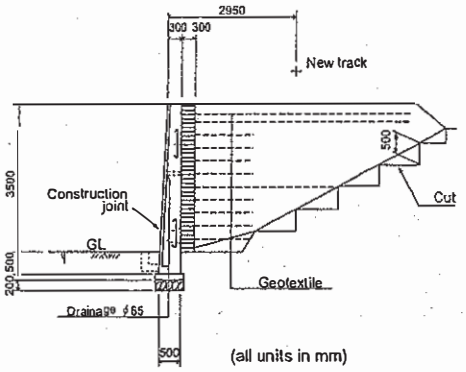

Fig.29 Typical cross-section of the RRR method wall

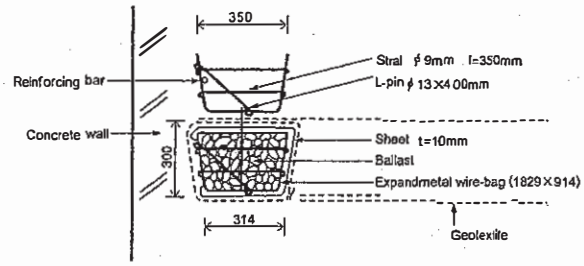

Fig.30 Metal-ware mesh gabions used at the shoulder of each soil layer

Table 3 Comparison of three methods for bridge abutment construction

	GRS-RW System	RC Frame structure
SKETCH	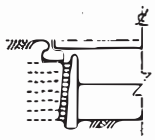	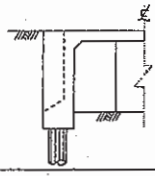
PLUSES	Large construction equipment is not used	Negligible settlement
MINUSES	Possibility of selllement when the backfill is not well compacted	Piles are needed, which makes the construction work difficult in a limited area
PERIOD	Relatively short	Relatively long
COST	Relatively low	Relatively high

method for the bridge abutment construction. Fig.31 shows the bridge abutment. It was estimated that the cost was reduced to about a half when compared with that for the conventional RC structures.

Since the bridge abutments which were constructed by RRR method to support a very busy and important railway were the first ones in Japan, the behavior during and after construction was carefully monitored (Fig.32). Some observations were reported by Tateyama and Murata (1993). Fig.32 shows the arrangements of instrumentation at one of the two abutments.

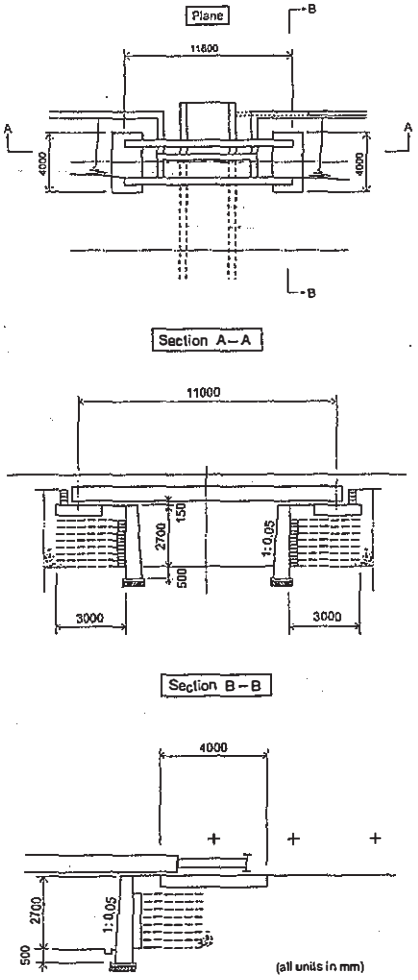

Fig.31 Plans and cross-sections of the bridge abutments at Takeshima BV

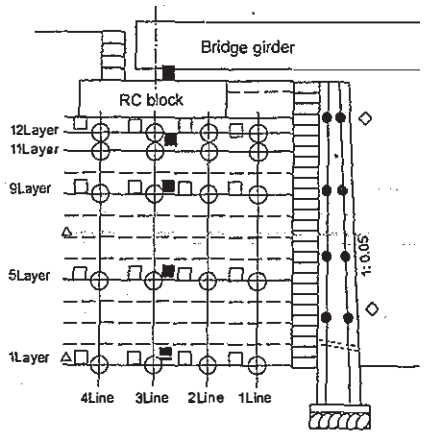

INSTRUMENTATION	NUMBER	LEGEND
Soil pressure	16	□
Acceleration	4	■
Void water pressure	2	△
Inclination	2	◇
Strain of geotextile	10	○
Strain of steel bar	8	●

Fig.32 Arrangements for measuring the performance of the bridge abutment at Takeshima BV

Fig.33 shows the increase in the vertical earth pressure and the axial strain in reinforcement recorded at the moment when the heaviest wheel load was above the abutment during passage of the first train. The maximum acceleration observed at the top of the abutment was about 0.2g and 0.1g in the vertical and horizontal directions. Relatively large strains were observed in the first and second reinforcement layers from the top. The maximum tension recorded was only about 0.5 kN/m, which is far bellow the tensile rupture strength. The earth pressure due to the train load decreased with the depth, while suggesting spreading at an angle of about 30^0 relative to the vertical. The distribution patterns of reinforcement force and earth pressure show that the reinforcement helped in supporting the train load. The observations obtained so far indicated that all the abutments by RRR method at the sites have been very stable.

Fig.34 shows the time history of the settlement at the concrete blocks supporting the railway girder placed on RRR method walls. The number of passing trains was, on average, about 250 times a day, while each train consists of about 8～12 cars with about

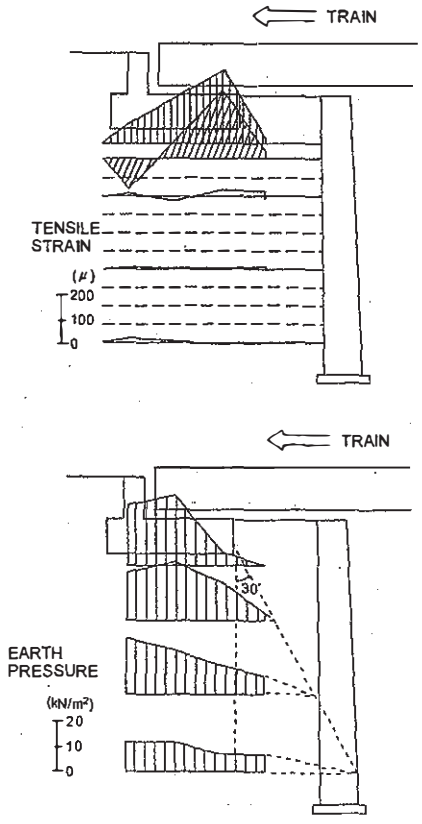

Fig.33 Increase in the strain in reinforcement and the earth pressure at several levels in GRS-RW bridge abutment

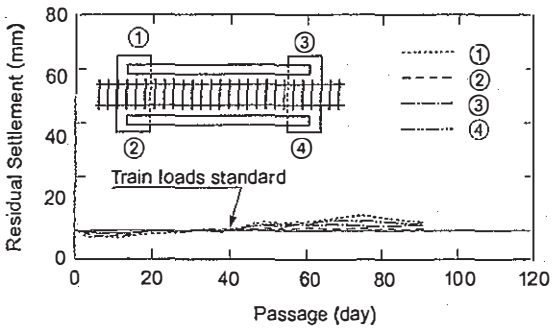

Fig.34 Time history of the settlement at the concrete block supporting the rail girder

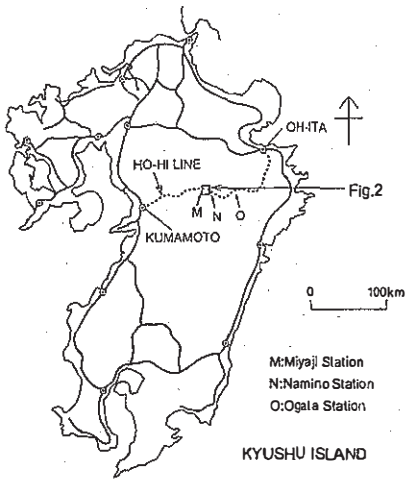

Fig.35 Location of the site

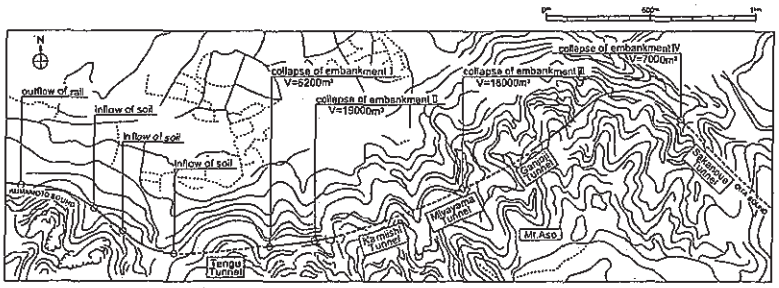

Fig.36 Plan of main damaged locations of Hohi-Line at Aso site

500 kN per car (n.b., about 120 kN per wheel). It may be seen from Fig.34 that after some initial settlement, developed during several days after the start of train passing, it virtually stopped increasing. The settlements due to train load observed at all the abutments by RRR method have been far less than allowable limit.

6.3 Aso Mountain Area Site (Emura et al., 1994)

In the central part of Kyushu Island, a series of full sections of railway embankments for a one-track railway Ho-Hi line had been washed away during a heavy rainfall on 2 July 1990. This railway had connected Oh-ita and Kumamoto Cities on the east and west coasts of Kyushu Island (Fig.35). The damaged sites were located at remote places in a series of deep narrow valleys in the inside slope of the world's largest volcanic crater of Mt. Aso (Fig.36). At these sites, the railway has a steep slope of 25/1000. In Fig.35, a series of dashed lines indicate the locations of tunnels.

Four embankments, numbered Ⅰ～Ⅳ in Fig.36, with a total length of 195 m and a total earth volume of about 50,000 m^3 were reconstructed, using RRR method. Fig.37 shows the three typical cross-sections of the reconstructed embankments. The largest height of embankment was about 30 to 35 m with the crest length of 40 m at site Ⅲ. The reconstruction of the embankments by RRR method resulted in large savings of cost and time. The railway was re-opened on 19th October 1992.

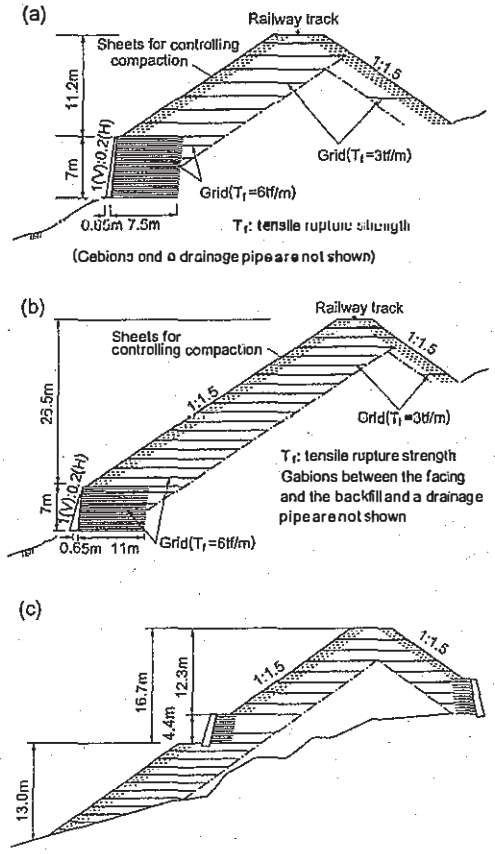

Fig.37 Three typical cross-sections of reconstructed embankment; (a) the site Ⅳ, (b) the site Ⅱ and (c) the site Ⅰ, Aso site

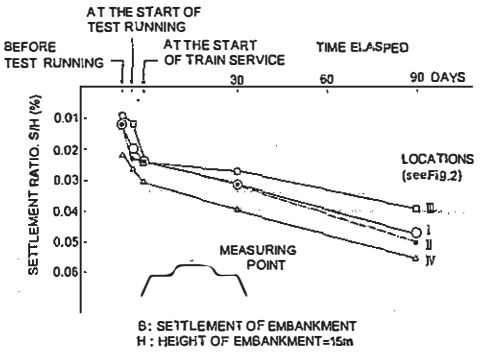

Fig.38 Typical record of the settlements at the crest of the embankment after the re-start of train passing (H=15m), the site I

After the completion of reconstruction, the settlement at the crests of embankment was measured for about three months after the re-opening of operation (Fig.38). It may be seen that a small settlement (2 ~4 mm) about 0.02% of the embankment height occurred immediately after the start of test running of trains. The settlement was not due to the deformation of the main body of embankment.

The additionally recorded settlement at the subsequent stages after the start of train passage has also been small, about 0.03% of the embankment height (about 4 mm). The total settlement so far was very small. Currently, the railway at the site is being operated without any problems.

6.4 Nagano Bullet Train Yard Sites (Kojima et al., 1996)

Hokuriku bullet train yard in Nagano is located 10 km north-east of Nagano station. The position of train yard is shown in Fig.39, plan of the site in Fig.40, and cross-section of the embankment in Fig.41. The train yard is designed approximately 100 m wide and 2 km long. The embankment is designed 2 m high from G.L.. West side off this embankment was built by RRR method and east side is slope.

This train yard is on a very soft ground formed by Chikuma River. The geological map is shown in Fig.42. This area is constituted of soft clay layer, over 20 m deep, in Quartenary Alluvium deposit. Layers can be seen form top to down: first Alluvium clay (Ac1 to Ac4: with peat and some thin sand layer), second Diluvial clay (Dc), and third Diluvial gravel (Dg), In these layers, soft (peat or clay) layers stretch 20 m deep from G.L.. The characters of this layer are N value: 0 to 3, natural water content: 40 to 200%, unconfined compressive strength: 20 to 80 kN/m^2, and random range of various values. Consolidation settlement had to be considered.

Much clay(weathered tuff) as the backfill materials was used for the first time in Japan. To hold down pore water pressure of embankment the reinforced materials composite geosynthetics, using clay as

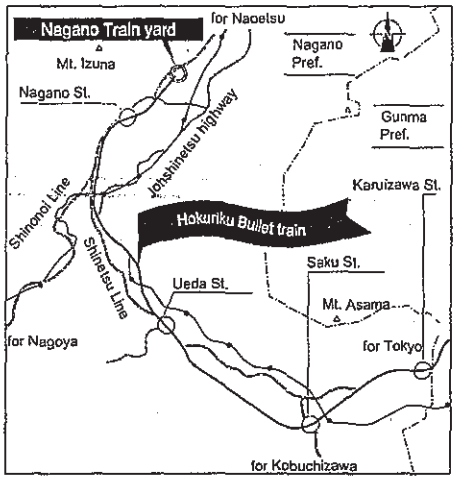

Fig.39 Position of train yard

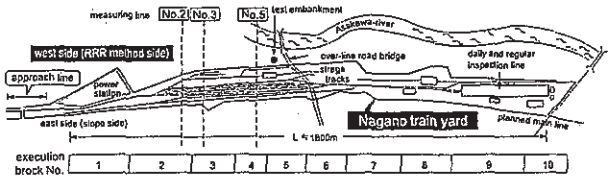

Fig.40 Plan of the site

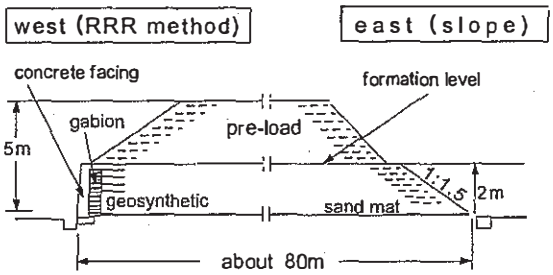

Fig.41 Cross-section of the embankment

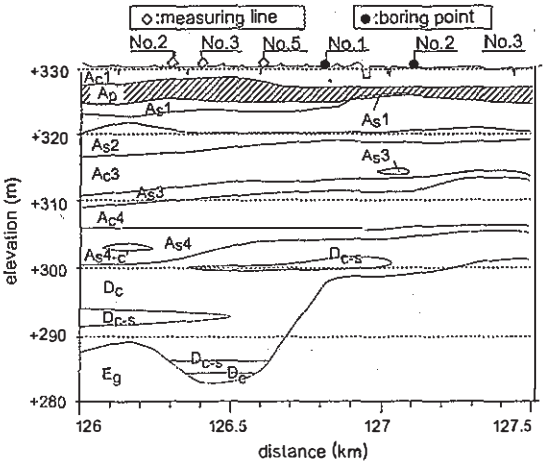

Fig.42 Geological map

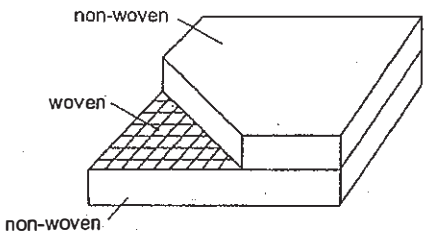

Fig.43 Composite geosynthetics

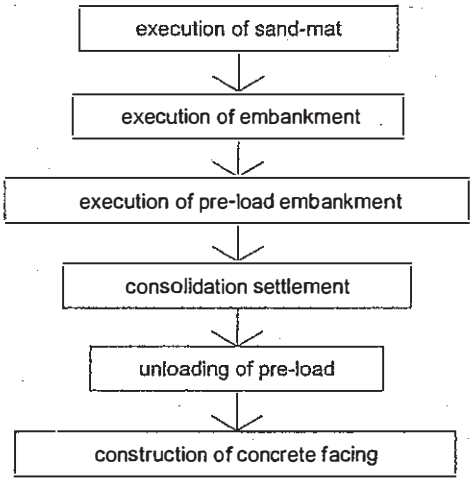

Fig.44 Process of execution

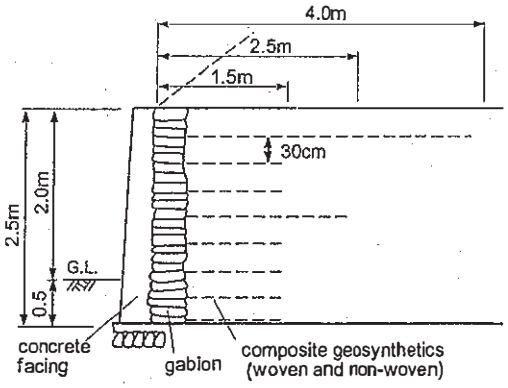

Fig.45 Cross-section of RRR method

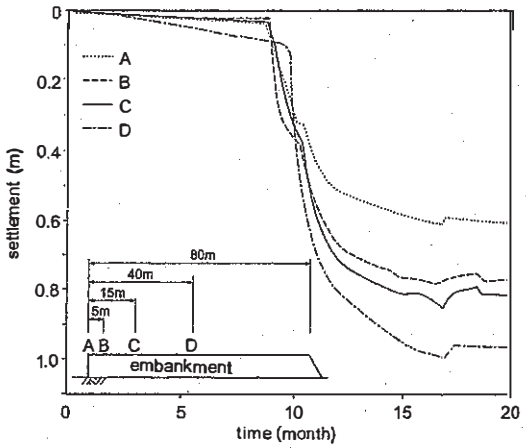

Fig.46 Settlement of ground surface

backfill materials is shown in Fig.43, were used. This geosynthetics from three layers, first and third layers are non-woven geosynthetics, second layer is woven geosynthetics. The geosynthetics give two effects i.e. reinforcement and drainage. Woven geosynthetics have reinforcement effect, and non-woven geosynthetics do drainage effect.

After investigation and planning, the area of train yard sank approximately 1 m due to the embankment, and consolidation settlement took 6 to 17 months to attain 90%. So consolidation settlement was examined. Pre-loading method, and sand drain method are generally known as the method for consolidation settlement. As pre-loading method has an economic advantage and it can hasten consolidation of the peat layer, the pre-loading method was proposed.

The embankment was constructed, dividing it into 10 parts since December 1993. Fig.44 shows the process of execution. The accelerated consolidation was used taking time until consolidation settlement finished before executing concrete facing for reason of a very soft ground.

Cross-section of this walls is shown in Fig.45. The geosynthetics 1.5 m long and 0.3 m high are used, and long geosynthetics are used in the fifth layer up to internal friction angle line. 2.5 m high walls were executed considering settlement and the pre-loading embankment 2.5 m high, slope rate: 1:1.5. Therefore total height of the embankment was 5.0 m. Reinforced concrete wall as retaining wall with rigid facing, was built after removing pre-loading embankment and achieving final settlement.

15 measuring lines were set every 100 m for execution management. Measured values of the measuring line No.3 was shown mainly. Horizontal displacement on this line was not measured, and only horizontal displacement line No.5 was shown. Settlement of the ground surface on the measuring line No.3 is shown in Fig.46. At the center of the embankment approximately 1 m consolidation settlement occurred in about 6 months. Settlement progressed faster then forecast. And it can be seen a decrease of settlement after removing the charge embankment. Settlement of each layer curve on the measuring line No.3 is shown in Fig.47. It can be seen that settlement goes as fast as settlement of Ap layer, accounting for large part of consolidation settlement. Cross-section of settlement on measuring line No.3 is shown in Fig.48. It can be seen settlement range from 0.35 to 1.0 m, but the ground surface shifts horizontally little and the point

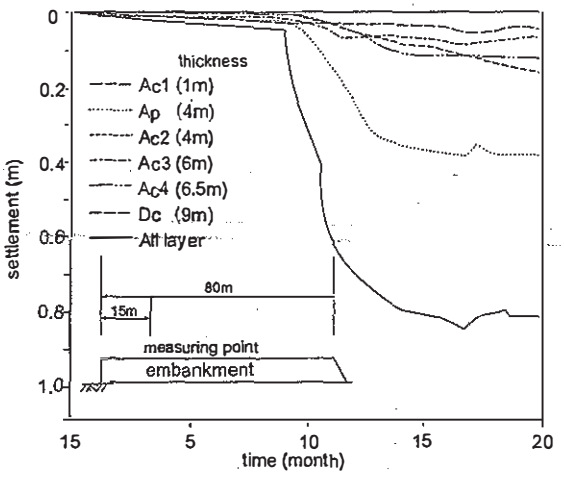

Fig.47 Settlement of each layer

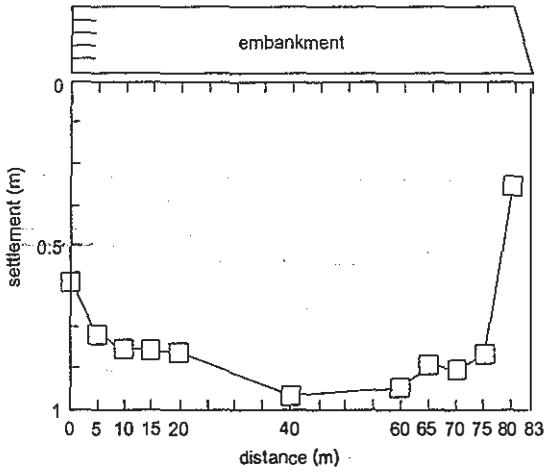

Fig.48 Cross-section of settlement

at 2 m to 3 m deep from G.L. shifts as much as 0.15 m. It seems that lateral flow of the walls are restricted by the geosynthetics of the bottom layer.

7 PERFORMANCE OF RRR METHOD DURING THE 1995 HYOGOKEN-NANBU EARTHQUAKE (Tatsuoka et al.,1995)

On the 17th of January,1995, a devastating earthquake measuring 7.2 in the Richter scale hit the southern part of Hyogo Prefecture including Kobe City and the neighbouring urban areas.

In the affected area, an extensive length of embankment had been constructed long time ago for JR Tohkaido Line of West Japan Railway (JR) Company, which is one of the most important railways in Japan, Kobe Line of Hankyuu Railway Company and Main Line of Hanshin Railway Company. About 60 years ago, in the central zone of Kobe City, a large length of them was replaced by elevated steel-reinforced concrete (RC) frame structures, which were seriously damaged by this earthquake. The railway embankments existing at the moment of this earthquake had a number of retaining walls (RWs) of old type in the high seismic intensity areas, and most of them were seriously damaged.

These RWs for railway embankments can be categorized into following five groups:

1) Masonry RWs,
2) Leaning-type (supported type) unreinforced concrete RWs,
3) Gravity-type unreinforced concrete RWs,
4) Cantilever-type or T-shaped type RC RWs
5) RRR method.

1) Masonry RWs:

This is the oldest type. Most of them were constructed more than about 70 years ago.

No seismic design was performed. They were on average most seriously damaged among all the types of RWs. Most of the RWs of this type located in the areas where the JMA scale (Japanese seismic intensity scale: for example seventh = a collapse ratio of wooden houses equal to 30% or more) was equal to seventh or higher were more-or-less damaged. Fig.49 shows a typical case, constructed 64 years ago. A stack of stones totally collapsed into stone pieces.

2) Leaning-type unreinforced concrete RW:

Most of them were constructed more than about 60 years ago. No seismic design was performed. Fig.50 shows a typical one, constructed 58 years ago to support the embankment for JR Tohkaido Line. Continuously for a large length, the RW was broken at the bottom and the upper part overturned completely to the ground showing the back face upside, which was perhaps triggered by both large horizontal seismic

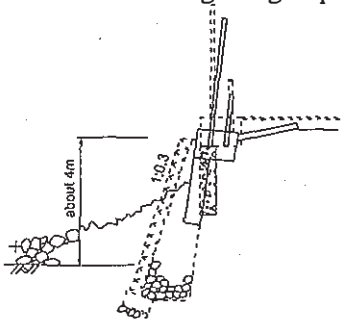

Fig.49 Typical damaged masonry RW; embankment along JR Tohkaido Line between Setsu-Motoyama and Sumiyoshi Stations

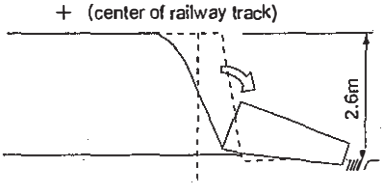

Fig.50 Typical damaged leaning-type unreinforced concrete RW; embankment along JR Tohkaido Line between Setsu-Motoyama and Sumiyoshi Stations

force worked to the RW itself and large seismic earth pressure exerted from the backfill. It seems, however, that the former should be the major factor for complete overturning, since the backfill soil did not move outwards following the movement of the RW.

3) Gravity-type unreinforced concrete RW:

Most of them were constructed more than about 60 years ago. Fig.51 shows the case of most serious damage, in which a length of RW tilted largely, while some section totally over-turned for a length of 200 m. These RWs were constructed 66 years ago based on the standard design, where pseudo-static stability analysis was adopted using a horizontal seismic coefficient of 0.2. It seems that their complete overturning was caused by large horizontal seismic force worked to them. These RWs of this type more-or-less tilted outwards considerably, which resulted in a large settlement at the crest of the railway embankment.

These there types of RWs described above are designed so that the gravity resistance of RW be large enough to resist against the lateral disturbing earth pressure exerted from the backfill. The damaged cases shown above and others indicate that these types of RWs had a very low seismic forces actually expected. It seems that even without seismic earth pressure applied to the backface, some of these RWs would have tilted or even completely over-turned. Construction of masonry or leaning-type RWs for important civil engineering structures is, therefore, not suggested (as specified in the current design standard for railway structures). A gravity-type unreinforced concrete RW having a very wide bottom would have been stable during this level of earthquake, but it is not practical.

4) Cantilever and inverted T-shaped RC RWs:

This is a rather modern type. They were aseismic designed. Fig.52 shows a typical damaged cantilever RC RW, constructed about 30 years ago, without using a pile foundation. The RW largely tilted outward inducing a large settlement at the crest of railway embankment. The footpath in front of the RW was pushed out laterally by this wall movement.

Shin-Nagata station of JR Sanyo Line was constructed about 30 years ago atop an embankment with the both sides being supported by a slope and this type of RW for a total length of about 800 m (Fig.53). It seems that this type of failure can be explained only by extra-ordinary large seismic earth pressure which resulted from the slope above the RW. Due to the failure of these RWs, Shin-Nagata station and the railway tracks at the site were seriously damaged.

5) RRR method

RRR method had been constructed at four locations for 1990-1994 in the affected area. RRR method with a total length about 2 km performed very

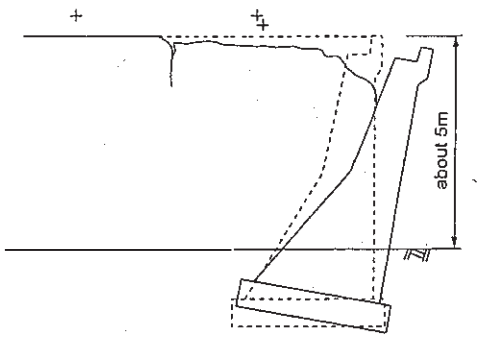

Fig.51 Typical damage to gravity-type unreinforced concrete RWs; embankment for Main Line of Hanshin Railway Co. adjacent to Ishiyagawa Station

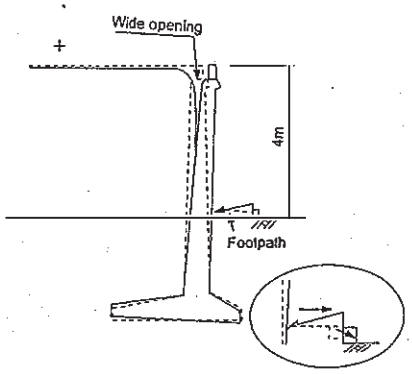

Fig.52 Typical damage to cantilever RC RWs for embankment of JR Sanyo Line between Hyogo and Shin-Nagata Stations

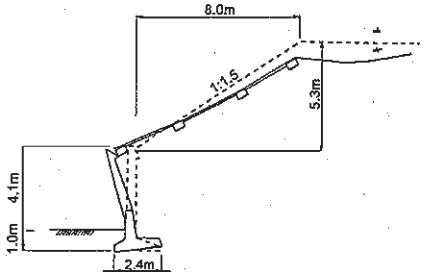

Fig.53 Rupture of the facing of cantilever RC RW; embankment of JR Shin-Nagoya Station

well. Among them, one constructed in 1992 at Tanata site was damaged only slightly, although it was located in one of the most shaken area.

Performance at Tanata site is shown bellow.

RRR method at Tanata site was completed in February 1992 on the south slope of the existing embankment of JR Tohkaido Line to increase the number of railway tracks from four to five (Fig.54c). At sections the wall became higher than 1.5 m, a series of H-shaped steel piles with some temporary anchors were provided to retain the embankment before some

part of the slope was excavated.

This wall deformed and moved slightly during the earthquake. Fig.53b shows the relative horizontal displacements between two adjacent facing sections at their top and bottom. The largest outward displacement occurred at the tallest part, in contact with a RC box culvert structure crossing the railway embankment, which was 26 cm and 10 cm at the top of the wall and at the ground surface level. The wall moved outward at the bottom by about 5 cm on average relative to the supporting ground, while pushing laterally the soil in front of the wall. Associated with the above, the railway track located above the reinforced zone of the backfill settled down about 15 cm at largest. This value was not particularly large when compared with that of the other three tracks located on the unreinforced zone of the embankment (Fig.54c). It seems that the settlement due to the dynamic compaction of the embankment body and ballast was also very large.

Despite the deformation and movement of the wall described above, the performance of RRR method is highly satisfactory when considering the following factors;

a) Extra-ordinary high seismic intensity at Tanata site:

The peak ground acceleration at Motoyama First Primary school, which is about 1 km west of Tanata, was extremely high, which can be inferred also from a very high collapse rate of Japanese wooden houses at the site (Fig.55). The totally collapsed wooden houses are not necessarily old, but many were constructed less than ten years ago. In the area surrounding Tanata site where the seismic intensity was estimated similar, or even less severe, the damage to many RC buildings and columns of high way and railway elevated RC frame structures was serious. In particular, the damage to many gravity-type RWs and cantilever RC RWs for railway structures was uncomparably more serious. It is certain that this RRR method experienced the highest seismic load among other modern geogrid-reinforced soil retaining walls.

b) Comparable performance of an adjacent RC RW (Fig.54e):

On the side opposite to the RRR method of the RC box structure, a RC RW with a largest height of about 6 m had been constructed concurrently with the RRR method, supported by a very good foundation of a row of bored piles. Although the ground

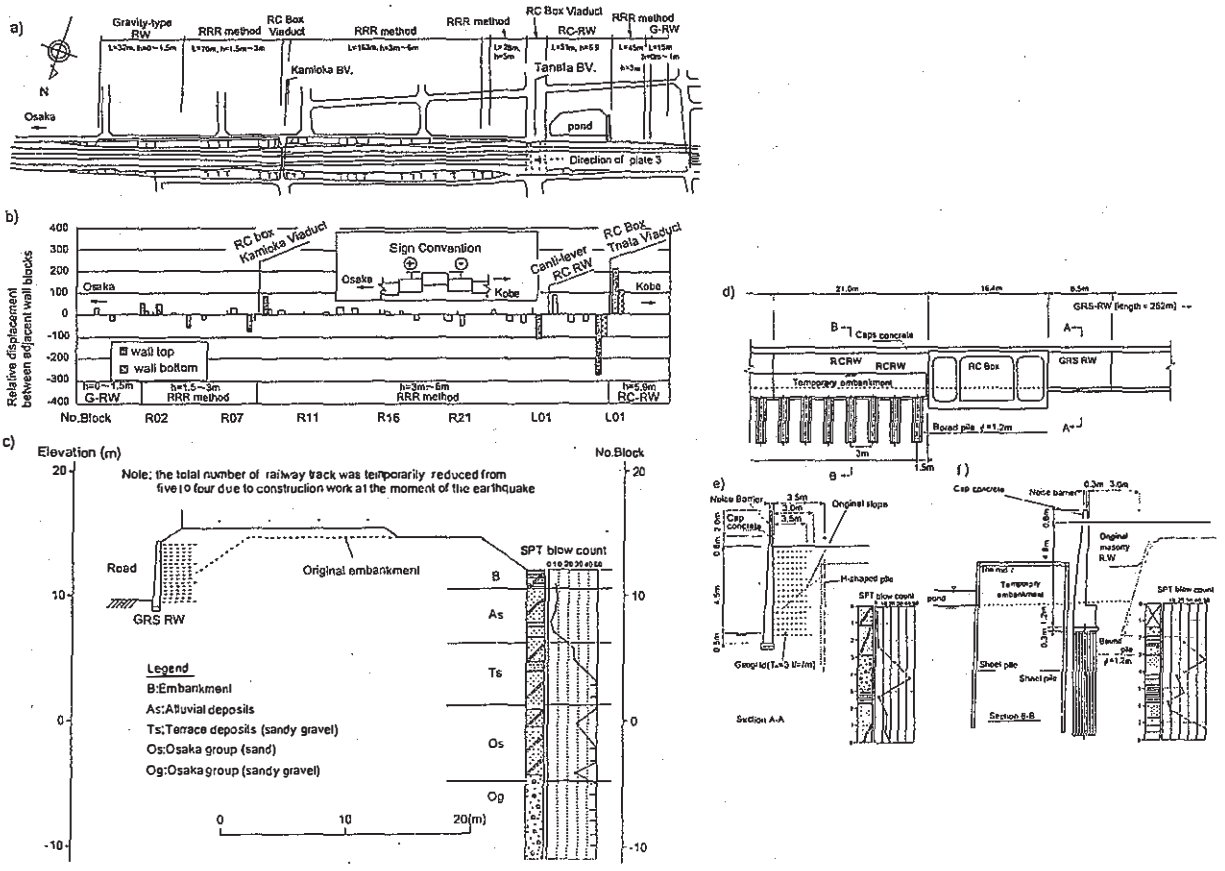

Fig.54 a) plan of the site, b)relative displacement between adjacent facing sections of RRR method and cantilever RC RW, c)cross-section of embankment, d) front view from south of GRS-RW and cantilever RC RW, e) typical cross-section of RRR method, and f) typical cross-section of RC RW at Tanata

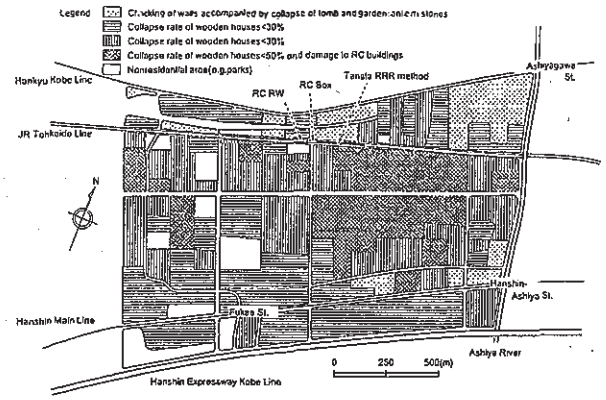

Fig.55 Details of the damage to wooden houses in the area in front of Tanata site

condition for the RC RW (Fig.54f) is similar to that for the RRR method (Fig.54e), it was decided to construct this pile foundation for the RC RW considering a relatively high water table. On the other hand, the RRR method is not supported by such a pile foundation. Consequently, the construction cost per wall length of the RC RW became nearly double as high as that for the RRR method. Besides, a temporary cofferdam still existed in front of the RC RW, which may somewhat contributed to the stability of the RC RW during the earthquake.

Despite the difference described above, the RC RW displaced similarly to the RRR method; i.e.., at the interface with the side of the RC box structure, the outward lateral displacement was 21.5 cm at the top and 10 cm at the ground surface level (Fig.54b).

c) Short reinforcement:

The length of geogrid reinforcement for this type of RRR method is in general shorter than that of metal strip-reinforced soil RWs. This results from much better pull-out resistance of grid and the contribution of a full-height rigid facing to the wall stability. Design Standard for Railway Earth Structures (1992) specifies the minimum allowable length of grid reinforcement for RRR method as the larger of 35% of the wall height and 1.5 m. For most of RRR method constructed so far, for conservatism, several top reinforcement layers were made longer than the others at lower levels (Fig.29). At Tanata site unfortunately the length of all the reinforcement layers were truncated to nearly a same length (Fig.53e), due to such a construction restraint as that the wall should be constructed while trains were running on the area to which the top several reinforcement layers should be extended. This arrangement may have reduced the seismic stability of the wall, the titling of the wall would have been smaller if the several top grid layers had been longer.

8 SHAKING TABLE TESTS AFTER THE 1995 HYOGOKEN-NANBU EARTHQUAKE

8.1 Shaking and Tilt Table Tests of Geosynthetic-Reinforced Soil And Conventional-Type Retaining Walls (Koseki et al, 1998)

A number of conventional masonry and unreinforced concrete gravity-type retaining walls for railway embankments were seriously damaged by the Hyogoken-nanbu Earthquake. Many modern cantilever-type, reinforced concrete (RC) retaining walls were also damaged, while RRR method performed well during the earthquake.

Considering the above situations, a series of shaking table tests was performed on relatively small-scale models of a geosynthetic-reinforced soil retaining wall with a full-height rigid facing (RRR method) and conventional type (gravity-type, leaning-type, and cantilever-type) retaining walls. Each model was subjected to horizontal uniform sinusoidal shakings at a frequency of 5 Hz. The initial base acceleration was set first to 50gals and increased at an increment of 50gals. Shaking was terminated when the wall displacement became considerably large.

The cross sections of five different model retaining walls are shown in Fig.56. The broken lines show the initial locations and the hatched zones show the displaced locations observed after failure of the model retaining wall. The total height of the walls was 530 mm except for the reinforced soil-type wall which was 500 mm high. The width of the base of the

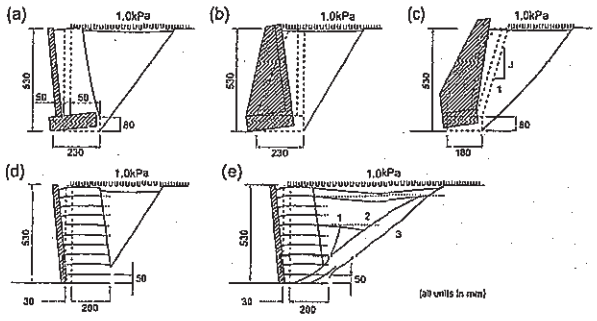

Fig.56 Initial and displaced locations and observed failure planes in the model retaining walls: (a) cantilever-type; (b) gravity-type; (c) learning-type ; (d) reinforced soil, Type 1; (e) reinforced soil, Type 2.

Table 4 Table model walls used in the shaking table tests

Model	Walltype	Surcharge on backfill (kPa)	Observed critical acceleration (gal)	Angle of the failure plane, β, observed at the end of test* (°)
S-2	Cantilever	1.0	430	55
S-3	Gravity	1.0	398	59
S-4	Leaning	1.0	301	51
S-5	Leaning	1.0	334	50
S-6	Leaning	1.0	319	49
S-7	Reinforced soil1	1.0	529	58
S-8	Reinforced soil2	1.0	654	70,53,40

cantilever-type and gravity-type walls was 230 mm, and it was reduced to 180 mm for the leaning-type wall. Ten layers of model reinforcement having a length of 200 mm were used for the reinforced soil, Type1 model walls. On the other hand, the length of the top and fourth layers were increased to 800 mm and 450 mm, respectively, for the reinforced soil, Type2 model wall in order to increase the stability against overturning, as is the common practice in Japan.

The configurations of the model walls used in the shaking table tests, and test results are summarized in Table 4.

For all of the models, the major failure mode of the walls was overturning as shown in Fig.56.

In order to compare the relative stability of different wall types, the observed critical seismic coefficient, $k_{h\text{-}cr(obs)}$, was defined as $k_{h\text{-}cr(obs)}=a_{cr}/g$, where a_{cr} is the amplitude of the base acceleration in the active state when the outward displacement at the top of the facing reached 5% of the total wall height (approximately 25 mm) and g is the gravitational acceleration.

In Fig.57, the observed critical seismic coefficients, $k_{h\text{-}cr(obs)}$, are compared with the predicted critical seismic acceleration coefficients, $k_{h\text{-}cr(cal)}$, which resulted in a factor of safety of unity against overturning for $\delta = 3/4\phi$ (δ : the wall friction angle. ϕ :the shear resistance angle).

For the cantilever-type, leaning-type, and gravity-type model walls, the observed values were almost equal to or smaller than the predicted values against overturning. The relative difference was larger in the order of the gravity-type, leaning-type, and cantilever-type walls. The smaller observed critical seismic coefficient for the gravity-type and leaning-type walls may be related to the inference that the interface friction angle δ_w activated along the virtually vertical back face within the backfill of the cantilever-type wall. On the other hand, the observed value was slightly larger than the predicted value for the reinforced soil, Type1 model wall, and noticeably larger for the reinforced soil, Type2 model wall.

The larger observed critical seismic coefficients for the reinforced-soil walls may be due to the difference in the location of center of rotation; i.e. the center of rotation moves away from the wall face into the backfill after the bearing capacity failure of the subsoil below the facing in the case of the gravity-type, leaning type, and cantilever-type walls. The distance of the same point of rotation from the back of the wall is less in the case of the reinforced soil walls due to the flexibility of the backfill.

It may also be seen from Fig.57 that the observed critical seismic coefficients for the different model walls scatter over a large range, while the corresponding values predicted by the pseudo-static stability analysis are within a relatively narrow range. This result indicates that the pseudo-static stability

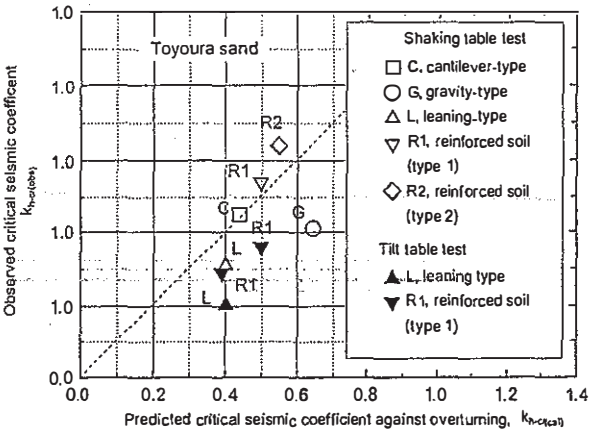

Fig.57 Comparison of the observed critical seismic coefficients, $k_{h\text{-}cr(obs)}$, to the predicted critical seismic coefficients, $k_{h\text{-}cr(cal)}$, against overturning, assuming $\delta=3/4\phi$

analysis cannot evaluate important aspects of the seismic stability of different types of walls. Particularly, the stability of the reinforced soil-type model walls in the shaking table test is underestimated by the current pseudo-static analysis in comparison with the gravity- and leaning-type retaining walls.

For the shaking table tests, the major observed failure mode was overturning with tilting of the wall face, which may have been triggered by a bearing capacity failure in the subsoil below the wall facing. The observed critical seismic coefficients were equal to or smaller than the predicted values against overturning for the cantilever-, gravity-, and leaning-type model walls. On the other hand, the observed critical seismic acceleration coefficient was slightly larger than the predicted value for the reinforced soil, Type1 model wall with reinforcement of equal length. Also, the ratio of the observed to predicted critical seismic acceleration coefficients was much larger for the reinforced soil, Type2 model wall which had longer reinforcement at higher wall levels.

These results suggest that ordinary pseudo-static seismic stability analysis based on the limit equilibrium method, used for the prediction of the critical seismic acceleration coefficients in the current study, underestimate the seismic stability of reinforced soil retaining walls in comparison with conventional, gravity-type soil retaining walls. These results are consistent with the observations of the seismic behavior of reinforced soil retaining walls (RRR method), conventional, reinforced concrete cantilever retaining walls, and conventional, gravity-type retaining walls during the 1995 Hyogoken-Nanbu Earthquake. These results also show that the long reinforcement layers placed at higher levels in the backfill can substantially increase the resistance against overturning failure. However, this contribution is not properly evaluated by the conventional stability analysis.

8.2 Irregular shaking table tests on seismic stability of reinforced-soil retaining walls (Watanabe et al., 2001)

In order to establish practical design procedures to evaluate seismic stability of different types of retaining walls(RWs) against high seismic loads, a series of shaking table tests with irregular wave were conducted on retaining wall models consisting of six different types. The cross-sections of six different model retaining walls are shown in Fig. 58. Seismic loads were applied by shaking the sand box horizontally with an irregular base acceleration which was recorded as N-S component during the 1995 Hyogoken-Nanbu earthquake. Its amplitude and time scale were adjusted so that the base acceleration has a prescribed maximum amplitude with a predominant frequency of 5 Hz.

Fig.59 shows the residual displacement of the wall(Gravity type RW & reinforced-soil RW type1) and the residual deformation of the backfill, which were observed at the end of final shaking step. For all RWs, the major failure pattern of the walls was overturning, which was associated with bearing capacity failure for the cantilever, leaning, and gravity type RWs.

For the reinforced-soil walls, no failure plane was observed at the bottom of the front wedge in the reinforced zone. The front wedge did not behave as rigid, but it suffered simple shear deformation along horizontal planes. This is because the resistance against the formation of failure plane penetrating though the reinforcement was larger than that against the simple shear deformation of the reinforced zone. This simple shear deformation of the reinforced backfill should be

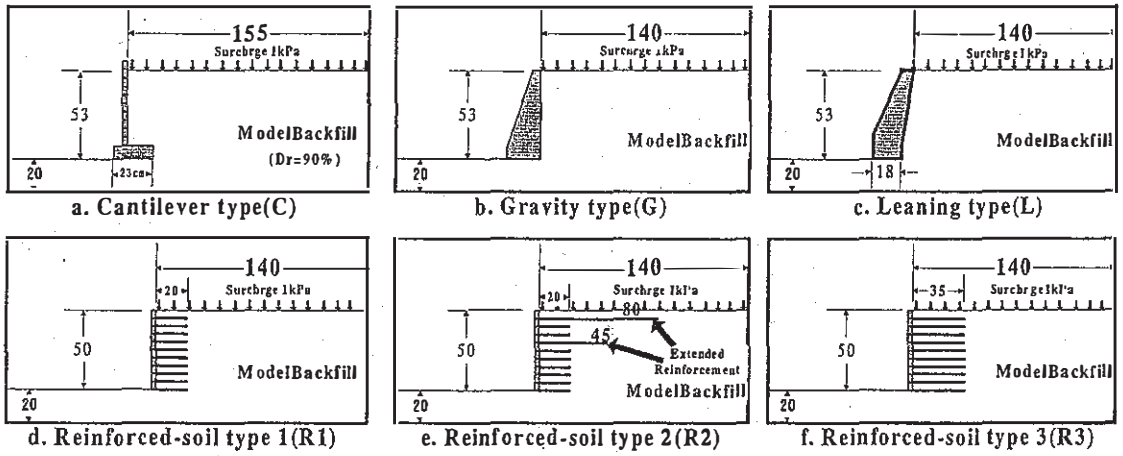

Fig.58 Cross-section of model retaining walls (unit in cm)

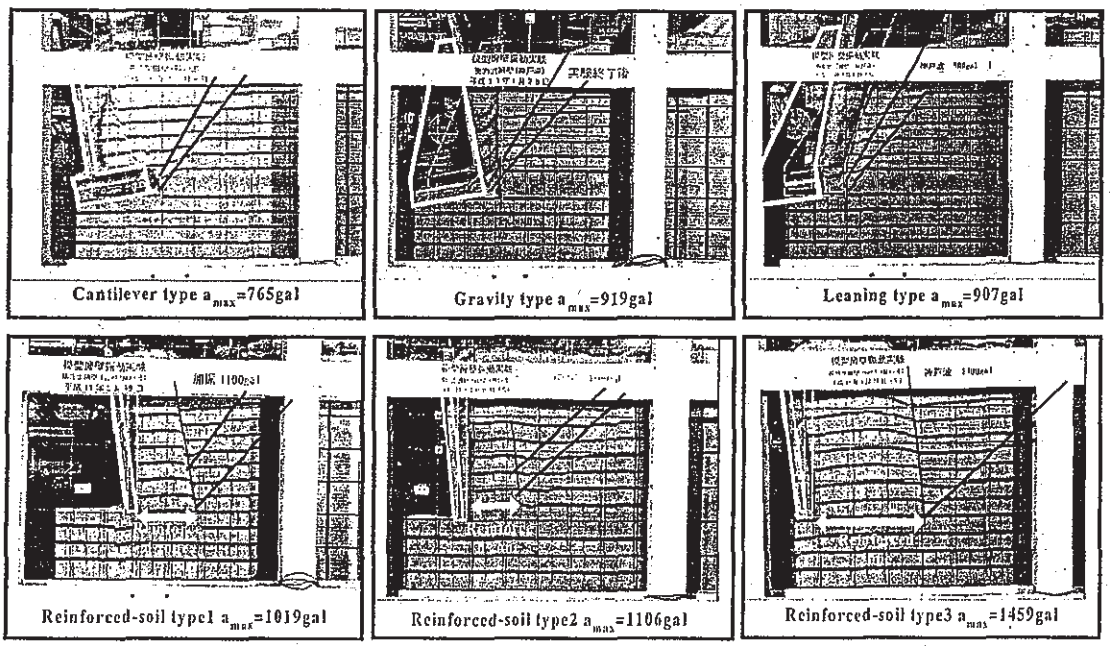

Fig.59 Residual displacement of the wall

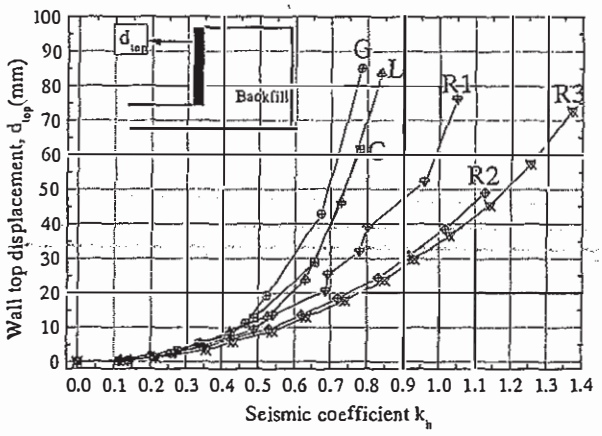

Fig.60 Accumulation of residual horizontal displacement near the top of the wall

considered to evaluate the residual displacement of the reinforced-soil RWs.

Fig.60 shows relationships between the seismic coefficient k_h and the horizontal displacement d_{top} at the end of each shaking step which was measured at a distance of 5cm below the top of the wall. The seismic coefficient k_h was defined as $k_h=a_{max}/g$, where a_{max} is the maximum base acceleration at the active state (i.e., when the inertia force was oriented towards the active direction) for each shaking step, and g is the gravitational acceleration. In the early steps of irregular shaking tests up to k_h value of about 0.5, the d_{top} value accumulated in a similar manner among different types of RWs. On the other hand, when the k_h value exceeded about 0.5, the rate of increase in the d_{top} value was larger for the three conventional type RWs than that for the reinforced-soil RWs. Further, though the total length of reinforcement of type2 was 80% as much as that of type 3, the seismic stability of them was on the same level. Such different extents of ductility in each type of RW agree with the damage observed after Hyogoken-Nanbu earthquake. This is caused by the different resistance mechanism against the external forces acting on the wall such as inertia force and seismic earth pressure.

The conventional type RWs resist against the overturning by the reaction force from subsoil. On the other hand, the reinforced-soil RWs resist against the overturning moment by the tensile force in the reinforcements in each layer. Fig.61 shows the relationship between the reaction force from subsoil and the horizontal displacement of the wall d_{top} for gravity type RW. In the early shaking steps, the normal stress measured at the toe of the base footing increased rapidly (①~⑥ in Fig. 61). After attaining the peak state, the d_{top} value suddenly increased due to loss of bearing capacity near the toe of the base footing(⑦~⑨ in Fig. 61). This behavior caused large decrease in the resisting moment against overturning, which led to the low ductility of conventional type RWs. Fig.62

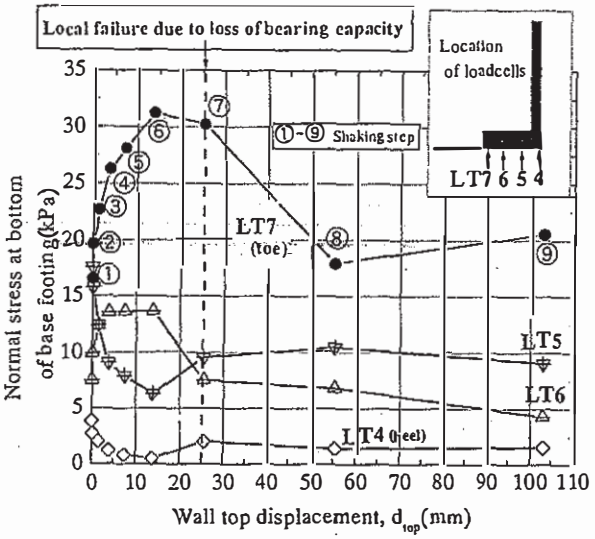

Fig.61 Measured reactions from subsoil for gravity type retaining wall

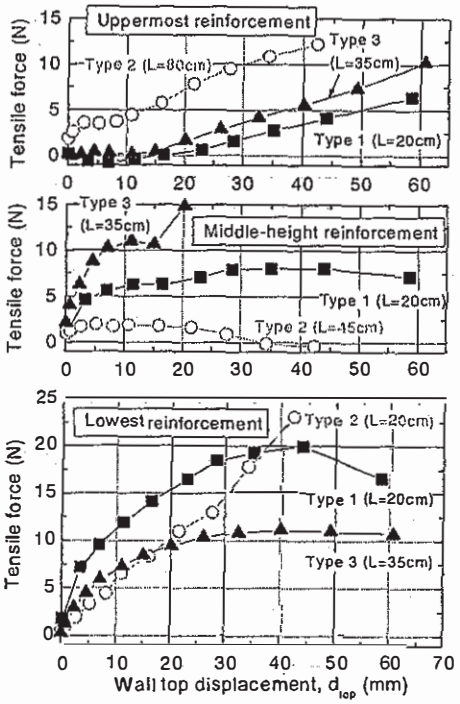

Fig.62 Tensile forces in reinforcement layers measured at a distance of 2.5cm from facing of reinforced-soil RWs

shows the relationship between the tensile force and the horizontal displacement of the wall d_{top}. For all types of reinforced-soil RWs, the tensile force increased with the d_{top} value, not showing such a sudden drop as observed in the reactions from subsoil for gravity type RW (Fig.61). This may explain the ductile behavior of reinforced-soil RWs.

Fig.63 shows the locations of failure plane and the

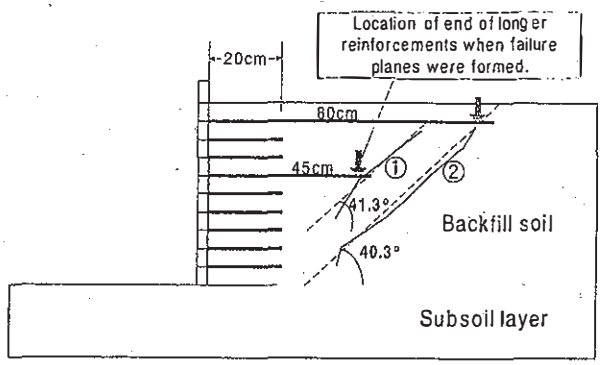

Fig.63 Comparison of locations of failure planes and longer reinforcement layers for reinforced-soil retaining wall type 2

reinforcements for reinforced-soil RW type 2. The arrows indicate the end of longer reinforcement at the moment when the failure planes were formed. The two failure planes were formed almost simultaneously. The upper one developed from the back of the reinforced zone towards just beside the end of the extended reinforcement(45cm), stopping somewhere below the longest reinforcement. On the other hand, the lower failure plane was formed just beside the end of the longest reinforcement(80cm) and reached the surface of the backfill. This demonstrates that the reinforcement resisted against the formation of the failure plane, and the location of the failure plane was strongly governed by the existence of the extended reinforcement. Accodingly large tensile force was mobilized in the extended reinforcements as shown in Fig 61, which lead to the high ductility of reinforced-soil RW type2.

9 CONCLUSIONS

The following conclusions may be derived from the laboratory test data and the field records for the geosynthetic-reinforced soil (GRS) retaining wall method presented in this report.

(1) The proposed method (RRR method), which uses short planar geosynthetic reinforcement and a continuous rigid facing, is a practical method to construct permanent retaining walls which can be used for important permanent structures including bridge abutments for high-speed railways. Recently this method has been used successfully for railway and road embankments at many sites in Japan. The total length of wall is now more than 50 km.

(2) The use of continuous rigid facing increases the stability of the wall, reduces the deformation of the wall against heavy rainfall, severe earthquake loading and dynamic train loading. And the use of continuous rigid facing increases the durability of the wall, and can provide a better appearance.

The proposed method (RRR method) located in severely shaken areas during the 1995 Hyogo-ken-Nanbu earthquake performed very well.

(3) A stage-construction method is suggested, in which a continuous rigid facing (e.g., delayed cast-in-place concrete facing) is placed directly over the wrapped-around face of the wall which has been constructed with the aid of gabions placed on the shoulder of soil layer.

This construction method is useful:

- for not damging the connection of reinforcing members to the back face fo facing that may be caused by the relative settlement between the facing and the backfill
- for developing tensile strains in reinforcing members during filling and compacting the backfill
- for not acivating too large earth pressure on the back face of facing during compaction of the backfill

(4) For a sandy backfill soil, the use of a grid-type geosynthetic is adequate. For a near-saturated cohesive backfill soil, the use of nonwoven-woven geotextile composite is suggested for better compaction of backfill soil, more efficient drainage from the interior of backfill, and more effective tensile-reinforcing.

REFERENCES:

Tatsuoka, F., Tateyama, M. and Murata, O. 1989. Earth retaining wall with a short geotextile and a rigid facing, Proc. 12th ICSMFE, 2: 1311-1314

Tatsuoka, F., Murata, O. and Tateyama, M. 1992, Permanent geosynthetic-reinforced soil retaining walls used for railway embankments in Japan, Geosynthetic-Reinforced Soil Retaining Walls, Wu(ed.), Balkema: 101-130

Murata, O., Tateyama, M. and Tatsuoka, F. 1992, Loading tests of geosynthetic-reinforced retaining walls and their stability analysis, Proc. Of Int. Sympo. On Earth Reinforcement Practice, IS Kyusyu '92, Fukuoka: 385-390

Murata, O., Tateyama, M. and Tatsuoka, F. 1994, Shaking table tests on a large geosynthetic-reinforced soil retaining wall model, Recent Case Histories of Permanent Geosynthetic-Reinforced Soil Retaining Walls, Tastuoka & Leshchinsky(eds.), Balkema: 259-264

Tateyama, M., Murata, O., Watanabe, K. and Tatsuoka, F. 1994, Geosynthetic-reinforced retaining walls for bullet train yard in Nagoya, Recent Case Histories of Permanent Geosynthetic-Reinforced Soil Retaining Walls, Tatsuoka & Leshchinsky(eds.), Balkema: 141-150

Horii,K., Kishida,H., Tateyama, M. and Tatsuoka,F.,1994, Computerized Design Method for Geosynthetic-Reinforced Soil Retaining Walls for Railway Embankmnets, Recent Case Histories of Permanent Geosynthetic-Reinforced Soil Retaining

Walls, Tatsuoka & Leshchinsky(eds.), Balkema: 205-218

Kanazawa, Y., Ikeda, K., Murata, O., Tateyama, M. and Tatsuoka, F. 1994, Geosynthetic-reinforced soil retaining walls for reconstructing railway embankment at Amagasaki, Recent Case Histories of Permanent Geosynthetic-Reinforced Soil Retaining Walls, Tastuoka & Leshchinsky(eds.), Balkema: 233-242

Tateyama, M . and Murata, O.,1993, Permanent geosynthetic-reinforced soil retaining walls used for bridge abutments, Proc. Of 13rd ICSMFE, New Delhi:1245-1248

Emura, Y., Tateyama, M. and Murata, O. 1994, Construction of geotextile-reinforced soil retaining walls to reconstruct railway embankment at Aso, Kyusyu, Recent Case Histories of Permanent Geosynthetic-Reinforced Soil Retaining Walls, Tastuoka & Leshchinsky(eds.), Balkema: 69-75

Kojima, K., Sakamoto, N., Tateyama, M. and Maruyama, O. 1996, Geosynthetic-reinforced soil retaining walls using clay on a very soft ground for Hokuriku bullet train yard in Nagano, Proc. Of Int. Sympo. On Earth Reinforcement Practice, IS Kyusyu '96, Fukuoka: 227-232

Tatsuoka, F., Koseki, J. and Tateyama, M. 1995, Performance of geogrid-reinforced soil retaining walls during the Greate Hanshin-Awaji Earthquake, January 17,1995, Earthquake Geotechnical Engineering, Ishihara(ed.), Balkema: 55-62

Koseki, J., Munaf, F., Tatsuoka, F., Tateyama, M., Kojima, K. and Sato, T. 1998, Shaking and tilt table tests of geosynthetic-reinforced soil and conventional-type retaining walls, Geosynthetics International' 1998, Vol.5: 73-96

Watanabe, K.., Tateyama, M., Kojima, K. and Koseki, J. 2001, Irregular shaking table tests on seismic stability of reinforced-soil retaining walls, Proc. Of Int. Sympo. On Earth Reinforcement Practice, IS Kyusyu '01, Fukuoka: